CFD STUDIES ON FLOW THROUGH COMPACT HEAT EXCHANGERS

A THESIS SUBMITTED IN PARTIAL FULFILLMENT OF THE REQIUREMENTS
FOR THE DEGREE OF

Bachelor of Technology
in
Mechanical Engineering

By

SOURAV MAZUMDAR
&
RAHUL SINGH

Department of Mechanical Engineering

National Institute of Technology

Rourkela

2007

CFD STUDIES ON FLOW THROUGH COMPACT HEAT EXCHANGERS

A THESIS SUBMITTED IN PARTIAL FULFILLMENT OF THE REQIUREMENTS
FOR THE DEGREE OF

Bachelor of Technology
in
Mechanical Engineering

By
SOURAV MAZUMDAR
&
RAHUL SINGH

Under the Guidance of

Prof. Sunil Kumar Sarangi

Department of Mechanical Engineering

National Institute of Technology

Rourkela

2007

National Institute of Technology
Rourkela

CERTIFICATE

This is to certify that the thesis entitled."CFD studies on flow through compact heat exchangers" submitted by Mr. Sourav Mazumdar and Rahul Singh in partial fulfillment of the requirements for the award of Bachelor of technology Degree in Mechanical Engineering at National Institute of Technology, Rourkela (Deemed University) is an authentic work carried out by him under my guidance .

To the best of my knowledge the matter embodied in the thesis has not been submitted to any University /Institute for the award of any Degree or Diploma.

Date:

Prof Sunil Kumar Sarangi
Dept. of Mechanical Engg.
National Institute of Technology
Rourkela-769008

Acknowledgement

We would like to express my deep sense of gratitude and respect to our supervisor Prof. Sunil Kumar Sarangi, for his excellent guidance, suggestions and constructive criticism. We consider ourselves extremely lucky to be able to work under the guidance of such a dynamic personality. His initiative of bringing FLUENT into our curriculum has given us an insight in CFD.

We would also like to thank Mr. Anil Kishan who gave us the fundamentals regarding FLUENT during May -2006 at NIT Rourkela. Besides we extend our gratitude to Prof A.K. Sathpathy for providing access to CFD Lab.Alongwith it we would like to thank Prof P.K. Rath and Prof S.K Mohapatra(ME) we also provided us many tips and suggestions which helped us to gain knowledge of CFD.

Lastly we would like to render heartiest thanks to our M.Tech students(ME) whose ever helping nature and suggestion has helped us to complete this present work.

Rahul Singh Sourav Mazumdar

CONTENTS

ABSTRACT

Plate fin heat exchangers, because of their compactness, low weight and high effectiveness are widely used in aerospace and cryogenic applications. This device is made of a stack of corrugated fins alternating with nearly equal number of flat separators known as parting sheets, bonded together to form a monolithic block. Appropriate headers are welded to provide the necessary interface with the inlet and the exit streams. While aluminum is the most commonly used material, stainless steel construction is employed in high pressure and high temperature applications.

The performance of a plate fin heat exchanger is determined, among other things, by the geometry of the fins. The most common fin configurations are - (1) plain (straight and uninterrupted) rectangular or trapezoidal fins (2) uninterrupted wavy fins and (3) interrupted fins such as offset strip, louver and perforated fins. The interrupted surfaces provide greater heat transfer at the cost of higher flow impedance.

The heat transfer and flow friction characteristics of plate fin surfaces are presented in terms of the Colburn factor j and the Fanning friction factor f vs. Reynolds number Re, the relationships being different for different surfaces. One of the earliest and the most authoritative sources for j and f data on plate fin surfaces is the monograph *Compact Heat Exchangers* by Kays and London [1984]. Although nearly two decades have passed after the latest edition, there has not been any significant addition to this database in open literature.

Unlike simpler geometries, the thermal performance of plate fin surfaces is not uniquely determined by the hydraulic diameter; other geometric variables such as fin spacing (s), fin height (h), fin thickness (t), offset strip length (l), wave length (Λ), and wave amplitude (a) have significant effect. It will be prohibitively expensive and time consuming to fabricate heat exchanger cores and carry out experiments over reasonable ranges of so many geometric variables. In contrast, it is reasonably easy and cost effective to conduct a parametric study in numerical simulation and derive correlations for use by the heat exchanger designer. But, because numerical solution is based on certain simplifying assumptions, the computed results are, in general, different from experimentally observed values. To alleviate this problem, we have evolved a procedure where some of the constants in the correlations are estimated from numerical simulation, the rest being determined by fitting experimental data

We have used the finite volume based CFD software, FLUENT 6.1 as the numerical tool. Three-dimensional, steady, Navier-Stokes equations and the Energy equation have been solved with appropriate boundary conditions for plain, offset strip and wavy fin surfaces. We have observed that the laminar flow model under predicts **j** and **f** values at high Reynolds number, while the 2-Layer k-e turbulence model over predicts the data throughout the range of interest. Because most industrial heat exchangers operate with Re less than 3000, and because the j and f data predicted by the laminar and the 2-layer k-e turbulence model differ little from each other at low Reynolds numbers, we have used the laminar flow model up to Reynolds number of 10,000, which is considered to be the limit for plate fin heat exchangers operating with gases. Velocity, pressure and temperature fields have been computed and **j** and **f** factors determined over appropriate range of Reynolds number and geometric dimensions. The **j** and **f** data have been expressed in the form:

$$j \text{ or } f = F(\text{Re, geometry})$$
$$= A\text{Re}^{b}\ \mathsf{F}\,(\text{dimensionless geometric parameters})$$

The function **F** is also a power law expression in the geometric parameters such as h/s, t/s, λ/s etc. We have determined the indices of **F** by multiple regression from numerically computed results, and the constants A and b by fitting experimental data of Kays and London. Because the **j** or **f** vs. Re curves show significant non-linearity, we have expressed the correlations in terms of two separate equations over the low and the high Re regimes. The transition Reynolds number has also been correlated with dimensionless geometric parameters.

We have thus carried out an exhaustive numerical study on the heat transfer and flow friction phenomena in plate fin heat exchanger surfaces with plain, wavy and offset strip fins. While the data for plain and offset-strip fins have been correlated successfully by pure power law expressions, those for wavy fins have demanded more complex relations. The indices of the dimensionless geometrical factors in wavy fin geometry have been expressed as simple polynomials of Reynolds number. A practical approach has evolved for determining the dependence of j and f factors on Re and dimensionless geometrical features.

A set of correlations has been generated for use in heat exchanger design. These correlations are expected to extend the range and accuracy of available correlations, particularly for offset strip fin and wavy fin surfaces.

Key words: Plate Fin Heat Exchanger, Heat Transfer Correlations, Plain Fin, Offset Strip Fin, Wavy Fin.

LIST OF GRAPHS

LIST OF TABLES

Chapter 1

INTRODUCTION

- Plate Fin Heat Exchangers
- Fin Geometries
- Flow Friction and Heat Transfer Characteristics
- Objectives of the Study

Plate fin heat exchangers are widely used in automobile, aerospace, cryogenic and chemical industries. They are characterized by high effectiveness, compactness (high surface area density), low weight and moderate cost. Although these exchangers have been extensively used around the world for several decades, the technologies related to their design and manufacture remain confined to a few companies in developed countries. Recently efforts are being made in India towards the development of small plate fin heat exchangers for cryogenic and aerospace applications. This thesis constitutes a part of this overall effort. Its focus, however, is on the basic heat transfer and flow friction phenomena applicable to all plate fin heat exchangers, and not confined to the Indian development programme.

Plate Fin Heat Exchangers

A plate fin heat exchanger is a form of compact heat exchanger consisting of a block of alternating layers of corrugated *fins* and flat separators known as *parting sheets*. A schematic view of such an exchanger is given in Fig. 1.1. The corrugations serve both as secondary heat transfer surface and as mechanical support against the internal pressure between layers.

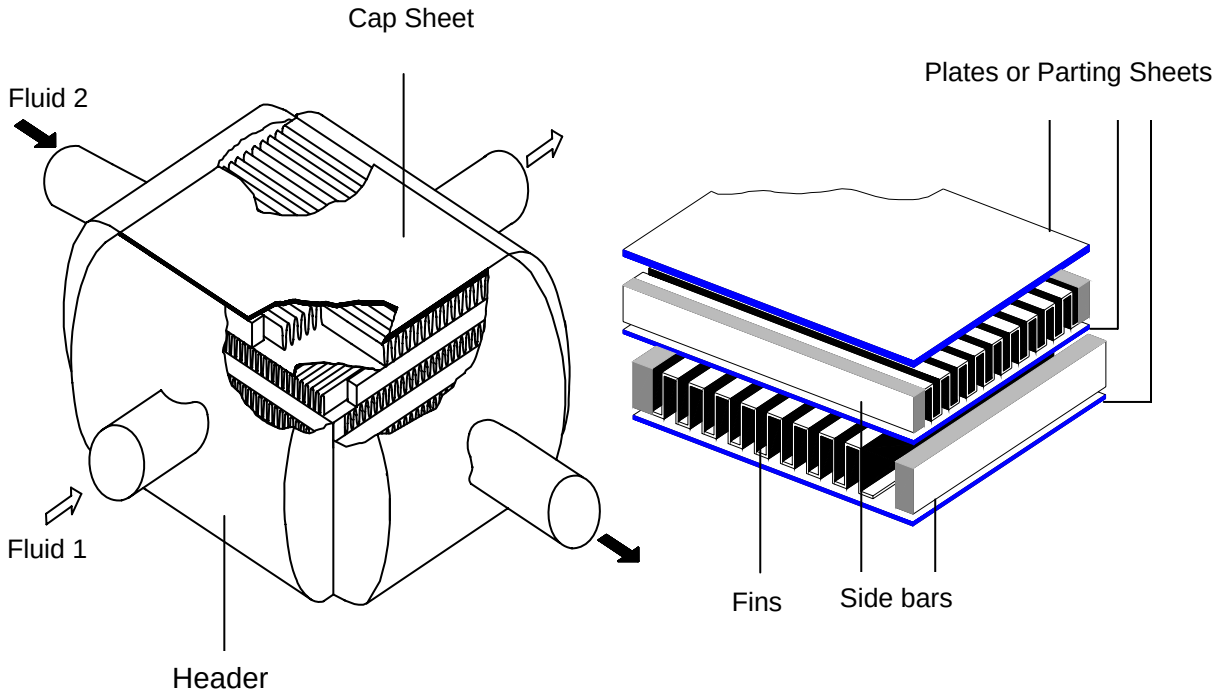

Figure 1.1: Plate fin heat exchanger assembly and details

Streams exchange heat by flowing along the passages

by the corrugations between the parting sheets. The edges of the corrugated layers are sealed by side-bars. Corrugations and side-bars are brazed to the parting sheets on both sides to form rigid pressure-containing voids. The first and the last sheets, called *cap sheets*, are usually of thicker material than the parting sheets to support the excess pressure over the ambient and to give protection against physical damage. Each stream enters the block from its own header via ports in the side-bars of appropriate layers and leaves in a similar fashion. The header tanks are welded to the side-bars and parting sheets across the full stack of layers.

Merits and Drawbacks

Plate fin heat exchangers offer several advantages over competing designs.

(1) High thermal effectiveness and close temperature approach. (Temperature approach as low as 3K between single phase fluid streams and 1K between boiling and condensing fluids is fairly common.),

(2) Large heat transfer surface area per unit volume (Typically 1000 m^2/m^3),

(3) Low weight,

(4) Multi-stream operation (Up to ten process streams can exchange heat in a single heat exchanger.), and

(5) True counter-flow operation (Unlike the shell and tube heat exchanger, where the shell side flow is usually a mixture of cross and counter flow.).

The principal disadvantages of the plate fin geometry are :

(1) Limited range of temperature and pressure,

(2) Difficulty in cleaning of passages, which limits its application to clean and relatively non-corrosive fluids, and

(3) Difficulty of repair in case of failure or leakage between passages

Materials

Plate fin heat exchangers can be made in a variety of materials. Aluminium is preferred in cryogenic and aerospace applications because of its low density, high thermal conductivity and high strength at low temperature. The maximum design pressure for brazed

aluminium plate fin heat exchangers is around 90 bar. At temperatures above ambient, most aluminium alloys lose mechanical strength. Stainless steels, nickel and copper alloys have been used at temperatures up to 500^0 C. The brazing material in case of aluminium exchangers is an aluminium alloy of lower melting point, while that used in stainless steel exchangers is a nickel based alloy with appropriate melting and welding characteristics.

Manufacture

The basic principles of plate fin heat exchanger manufacture are the same for all sizes and all materials. The corrugations, side-bars, parting sheets and cap sheets are held together in a jig under a predefined load, placed in a furnace and brazed to form the plate fin heat exchanger block. The header tanks and nozzles are then welded to the block, taking care that the brazed joints remain intact during the welding process. Differences arise in the manner in which the brazing process is carried out. The methods in common use are salt bath brazing and vacuum brazing. In the salt bath process, the stacked assembly is preheated in a furnace to about 550^0 C, and then dipped into a bath of fused salt composed mainly of fluorides or chlorides of alkali metals. The molten salt works as both flux and heating agent, maintaining the furnace at a uniform temperature. In case of heat exchangers made of aluminium, the molten salt removes grease and the tenacious layer of aluminium oxide, which would otherwise weaken the joints. Brazing takes place in the bath when the temperature is raised above the melting point of the brazing alloy. The brazed block is cleansed of the residual solidified salt by dissolving in water, and then thoroughly dried.

In the vacuum brazing process, no flux or separate pre-heating furnace is required. The assembled block is heated to brazing temperature by radiation from electric heaters and by conduction from the exposed surfaces into the interior of the block. The absence of oxygen in the brazing environment is ensured by application of high vacuum (Pressure $\approx 10^{-6}$ mbar). The composition of the residual gas is further improved (lower oxygen content) by alternate evacuation and filling with an inert gas as many times as experience dictates. No washing or drying of the brazed block is required. Many metals, such as aluminium, stainless steel, copper and nickel alloys can be brazed satisfactorily in a vacuum furnace.

Applications

Plate-fin and tube-fin heat exchangers have found application in a wide variety of industries. Among them are air separation (production of oxygen, nitrogen and argon by low temperature distillation of air), petro-chemical and syn-gas production, helium and hydrogen liquefiers, oil and gas processing, automobile radiators and air conditioners, and environment control and secondary power systems of aircrafts. These applications cover a wide variety of heat exchange scenarios, such as:

(1) exchange of heat between gases, liquids or both,

(2) condensation, including partial and reflux condensation,

(3) boiling,

(4) sublimation, and

(5) heat or cold storage

Flow Arrangement

A plate fin heat exchanger accepts two or more streams, which may flow in directions parallel or perpendicular to one another. When the flow directions are parallel, the streams may flow in the same or in opposite sense. Thus we can think of three primary flow arrangements – (i) parallel flow, (ii) counterflow and (iii) cross flow. Thermodynamically, the counterflow arrangement provides the highest heat (or cold) recovery, while the parallel flow geometry gives the lowest. The cross flow arrangement, while giving intermediate thermodynamic performance, offers superior heat transfer properties and easier mechanical layout. Under certain circumstances, a hybrid cross – counterflow geometry provides greater heat (or cold) recovery with superior heat transfer performance. Thus in general engineering practice, plate fin heat exchangers are used in three configurations: (a) cross flow, (b) counterflow and (c) cross-counter flow.

(a) Cross flow (Fig. 1.2(a))

In a cross flow heat exchanger, usually only two streams are handled, thus eliminating the need for distributors. The header tanks are located on all four sides of the heat exchanger core, making this arrangement simple and cheap. If high effectiveness is not necessary, if the two streams have widely differing volume flow rates, or if either one or both streams are

nearly isothermal (as in single component condensing or boiling), the cross flow arrangement is preferred. Typical applications include automobile radiators and some aircraft heat exchangers.

(b) Counter flow (Fig. 1.2 (b))

The counterflow heat exchanger provides the most thermally effective arrangement for recovery of heat or cold from process streams. Cryogenic refrigeration and liquefaction equipment use this geometry almost exclusively. The geometry of the headers and the distributor channels is complex and demands proper design.

(c) Cross-Counter flow (Fig.1.2 (c))

The cross-counterflow geometry is a hybrid of counterflow and cross flow arrangements, delivering the thermal effectiveness of counterflow heat exchanger with the

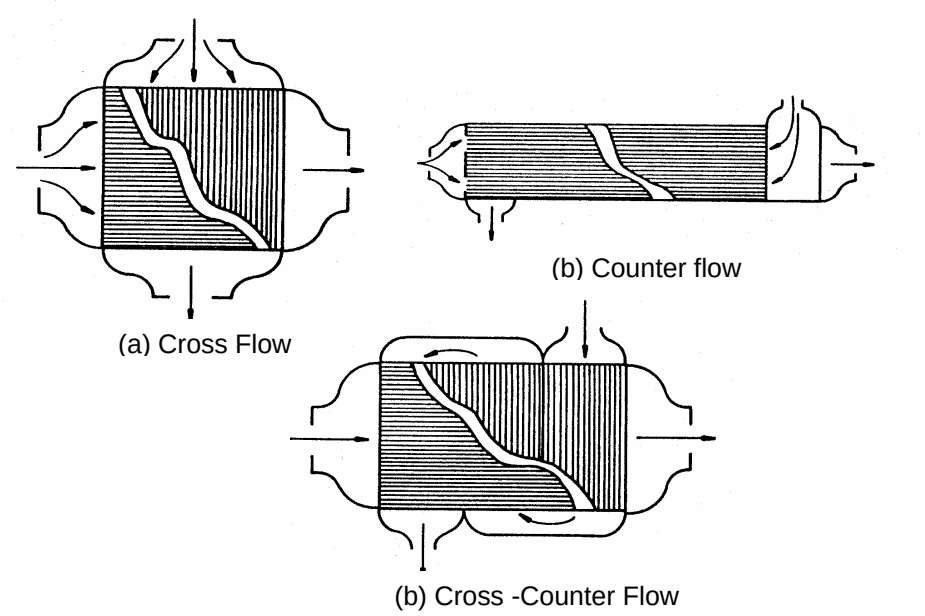

Figure 1.2: Heat exchanger flow arrangements

superior heat transfer characteristics of the cross flow configuration. In this arrangement, one of the streams flows in a straight path, while the second stream follows a zigzag path normal to that of the first stream. Up to six such passes have been employed. While negotiating the zigzag path, the fluid stream covers the length of the heat exchanger in a direction opposite to that of the direct stream. Thus the flow pattern can be seen to be globally counterflow while remaining locally cross flow. Cross-counter flow PFHEs are used in applications similar to those of simple cross flow exchangers, but allow more flexibility in design. They are particularly suited to applications where the two streams have considerably different volume flow rates, or permit significantly different pressure drops. The fluid with the larger volume flow rate or that with the smaller value of allowable pressure drop flows through the straight channel, while the other stream takes the zigzag path. For example, in a liquid-to-gas heat exchanger, the gas stream with a large volume flow rate and low allowable pressure drop is assigned the straight path, while the liquid stream with a high allowable pressure drop flows normal to it over a zigzag path. This arrangement optimises the overall geometry.

1.2 Fin Geometries

The performance of a plate fin heat exchanger is determined, among other things, by the geometry of the fins. The most common fin configurations are – (1) plain (straight and uninterrupted) fins with rectangular, trapezoidal or triangular passages, (2) uninterrupted wavy fins and (3) interrupted fins such as offset strip, louvered, perforated and pin fins. The details of each fin type are given below.

Plain Fins

These are straight fins that are continuous in the fluid flow direction (Fig.1.3(a, b). Although passages of triangular and rectangular cross section are more common, any desired shape can be given to the fins, considering only manufacturing constraints. Straight fins in triangular arrangement can be manufactured at high speeds and hence are less expensive than rectangular fins. But generally they are structurally weaker than rectangular fins for the same passage size and fin thickness. They also have lower heat transfer performance compared to rectangular fins, particularly in laminar flow.

Plain fins are used in those applications where core pressure drop is critical. An exchanger with plain fins requires a smaller flow frontal area than that with interrupted fins for specified pressure drop, heat transfer and mass flow rate. Of course, the required passage length is higher leading to a larger overall volume.

Wavy Fins

Wavy fins are uninterrupted fin surfaces with cross-sectional shapes similar to those of plain fins, but with cyclic lateral shifts perpendicular to the flow direction (Fig.1.3 (c)). The resulting wave form provides effective interruptions and induces a complex flow field. Heat transfer is enhanced due to creation of Goertler vortices. These counter-rotating vortices form while the fluid passes over the concave wave surfaces, and produce a corkscrew-like flow pattern.

The heat transfer and pressure drop characteristics of a wavy fin surface lie between those of plain and offset strip fins. The friction factor continues to fall with increasing Reynolds number. Wavy fins are common in the hydrocarbon industry where exchangers are designed with high mass velocities and moderate thermal duties. Unlike offset strip fins, the thickness of wavy fins is not limited at high fin densities. Therefore, wavy fins are often used for streams at high pressure, particularly those which can tolerate somewhat poor heat transfer coefficient.

Offset Strip Fins

This is the most widely used fin geometry in high performance plate fin heat exchangers. It consists of a type of interrupted surface, which may be visualised as a set of plain fins cut normal to the flow direction at regular intervals, each segment being offset laterally by half the fin spacing (Fig. 1.3 (d)). Surface interruption enhances heat transfer by two independent mechanisms. First, it prevents the continuous growth of thermal boundary layer by periodically interrupting it. The thinner boundary layer offers lower thermal resistance compared to continuous fin types. Above a critical Reynolds number, interrupted surfaces offer an additional mechanism of heat transfer enhancement. Oscillations in the flow field in the form of vortices shed from the trailing edges of the interrupted fins enhance local heat transfer by continuously bringing in fresh fluid

towards the heat transfer surfaces. This enhancement is accompanied by an increase in pressure drop.

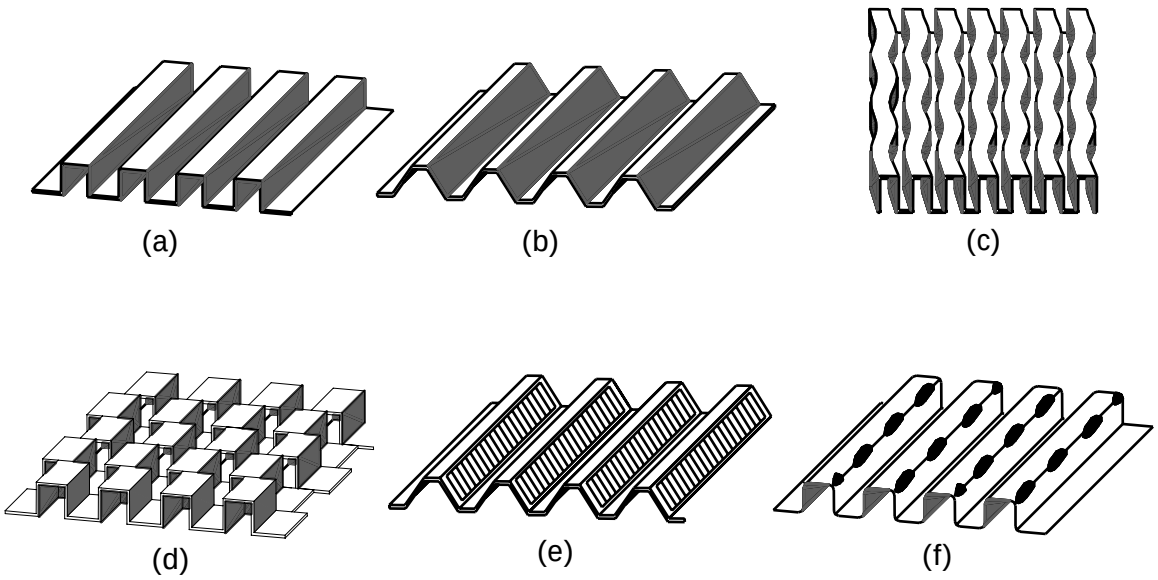

Figure 1.3: Types of plate fin surfaces: (a) plain rectangular (b) plain trapezoidal (c) wavy (d) serrated or offset strip fin (e) louvered (f) perforated

The heat transfer performance of offset strip fin is often as much as 5 times that of a plain fin surface of comparable geometry, but at the expense of higher pressure drop. For specified heat transfer and pressure drop requirements, the offset strip fin surface demands a somewhat higher frontal area compared to those with plain fin, but results in a shorter flow length and lower overall volume. An undesirable characteristic of this type of fin is that at high Reynolds numbers the friction factor remains nearly constant (because of the higher contribution of form drag), while the heat transfer performance goes down. Therefore, offset strip fins are used less frequently in very high Reynolds number applications. On the other hand, they are extensively used in air separation and other cryogenic applications where mass velocities are low and high thermal effectiveness is essential.

Other Fin Types

The louvered fin geometry shown in Fig. 1.3 (e) bears a similarity to the offset strip fin. Instead of shifting the slit strips laterally, small segments of the fin are slit and rotated 20 to 45 degrees relative to the flow direction. The base surface of the louvered fin geometry can be of triangular or rectangular shape, and louvers can be cut in many different forms.

The multilouvered fin has the highest heat transfer enhancement relative to pressure drop in comparison with most other fin types. Flow over louvered fin surfaces is similar in nature to that through the offset strip fin geometry, with boundary layer interruption and vortex shedding playing major roles. An important aspect of louvered fin performance is the degree to which the flow follows the louver. At low Reynolds number the flow is nearly parallel to the axial direction (duct flow), whereas at high Reynolds number the flow is in the direction of the louvers (boundary layer flow). Louvered fins are extensively used in automotive heat exchangers.

Perforated fins shown in Fig.1.3 (f) are made by punching a pattern of spaced holes in the fin material before it is folded to form the flow channels. The channels may be triangular or rectangular in shape with either round or rectangular perforations. While this geometry, with boundary layer interruptions, is a definite improvement over plain fins, its performance is generally poorer than that of a good offset strip fin. Furthermore, the perforated fin represents a wasteful way of making an enhanced surface, since the material removed in creating the perforations is thrown out as scrap. Perforated fins are now used only in limited number of applications such as turbulators in oil coolers.

In a pin fin exchanger, a large number of small pins are sandwiched between plates in either an inline or staggered arrangement. Pins may have a round, an elliptical, or a rectangular cross section. These types of finned surfaces are not widely used due to low compactness and high cost per unit surface area compared to multilouvered or offset strip fins. Due to vortex shedding behind the pins, noise and flow-induced vibration are produced, which are generally not acceptable in most heat exchanger applications. The potential application of pin fin surfaces is at low flow velocities ($Re < 500$), where pressure drop is negligible. Pin fins are used as electronic cooling devices with free-convection flow on the pin fin side.

1.3 Heat Transfer and Flow Friction Characteristics

The heat transfer and flow friction characteristics of a heat exchanger surface are commonly expressed in non-dimensional form and are simply referred to as the basic characteristics or basic data of the surface. These characteristics are presented in terms of the Colburn factor **j** and Friction factor **f** vs. Reynolds number Re, the relationships being different for different surfaces. The Colburn and Friction factors are defined by the relations:

$$\mathbf{j} = \frac{h}{GC_p}(Pr)^{\frac{2}{3}} \tag{1.1}$$

$$\Delta p = \frac{4\,\mathbf{f}\,L\,G^2}{2D_h\rho} \tag{1.2}$$

where, h = heat transfer coefficient ($W/m^2\,K$)

G = mass velocity (kg/m^2s) [on the basis of minimum free flow area]

L = length of flow passage (m)

D_h = hydraulic diameter (m), and

ρ = mean density of fluid (kg/m^3).

The friction factor **f** takes both viscous shear (skin friction) and pressure forces (form drag) into consideration. This approach is somewhat arbitrary since geometric variables, other than the hydraulic diameter, may have a significant effect on surface performance. It also becomes necessary to present j and f data separately for each surface type. The **j** and **f** data so presented are applicable to surfaces of any hydraulic diameter, provided a complete geometric similarity is maintained.

One of the earliest and the most authoritative sources of experimental **j** and **f** data on plate fin surfaces is the monograph *Compact Heat Exchangers* by Kays and London [1]. Although nearly two decades have passed after the latest edition, there has not been any significant addition to this database in open literature. Attempts have been made towards numerical prediction of heat transfer coefficient and friction factor; but they have generally been unable to match experimental data. Several empirical correlations, however, have been generated from the data of Kays and London, which have found extensive application in industry, particularly in less-critical designs. For critical applications, direct experimental determination of **j** and **f** factors for each fin geometry remains the only choice.

In a plate fin heat exchanger, the hydraulic diameter of the flow passage is generally small due to closely spaced fins. Operation with low density gases leads to excessive pressure drop unless the gas velocity in the flow passage is kept low. These factors imply operational Reynolds number less than 10,000, the common range being between 500 and 3000 for most ground based applications

1.4 Objectives of the Study

The objectives of the present study are to simulate the flow and temperature fields in plate fin heat exchanger passages and to establish heat transfer and flow friction correlations covering a wide range of finned surfaces. Unlike simpler geometries, the performance of a plate fin surface is not uniquely determined by the hydraulic diameter. Other geometric parameters such as fin spacing (s), fin height (h), fin thickness (t), offset strip length (l), wave length (Λ), and wave amplitude (a) etc play significant roles. It will be prohibitively expensive and time consuming to fabricate heat exchanger cores and conduct experiments over reasonable ranges of all the geometric variables. In contrast, it is relatively easy and cost effective to carry out a parametric study through numerical simulation and derive acceptable correlations for use by the heat exchanger industry. But, because numerical solution is based on certain simplifying assumptions, the computed results are, in general, different from experimentally observed values. To circumvent this problem, we have evolved a procedure where some of the constants in the correlations are estimated from numerical simulation, the rest being determined by fitting experimental data. We have thus taken advantage of both experimental and numerical tools, and feel that this method gives the most practical approach to finding heat transfer and flow friction correlations for complex surfaces.

We have used the finite volume based CFD software FLUENT 6.1 as the numerical tool for computing the flow and temperature fields. Three-dimensional, steady Navier-Stokes (continuity and momentum conservation) and Energy equations have been solved with

appropriate boundary conditions for plain, offset strip and wavy fin surfaces. We have observed that the laminar flow model under predicts **j** and **f** values at high Reynolds number.. Because most industrial plate fin heat exchangers operate with Re less than about 3000, the laminar flow model appears to be the most appropriate. We have used the laminar flow model up to Reynolds number of 10,000, which is considered to be the limit for plate fin heat exchangers operating with gases. Velocity, pressure and temperature fields have been computed and **j** and **f** factors determined over appropriate ranges of Reynolds number and geometric dimensions. The friction factor **f** is based on static pressure drop over the total length for plain fins and over the periodic length for offset strip and wavy fins. The j **and** f data have been expressed in the form:

$$\mathbf{j} \text{ or } \mathbf{f} = F(\text{Re, geometry})$$
$$= A\,\text{Re}^{b}\,F(\text{dimensionless geometric parameters})$$

We have chosen the function F in the form of a power law expression in dimensionless geometric parameters h/s, t/s, λ/s, Λ/s and a/s etc as appropriate for the chosen fin geometry. We have determined the indices of F by multiple regressions from numerically computed results, and the constants A and b by fitting experimental data of Kays and London. For the flow friction correlations, we have also used some experimental data generated recently in our own laboratory. Because the **j** and **f** vs. Re curves show significant non-linearity, we have expressed the correlations in terms of two separate equations over the low and the high Re regimes. The transition Reynolds number has also been correlated with dimensionless geometric parameters.

Chapter 2

Plain Fin Surfaces

- The Plain Fin Geometry
- Computational Domain, Boundary Conditions and Numerical Model
- Velocity and Temperature Fields
- Computation of j and f factors
- Role of Reynolds Number and Geometric parameters

The plain rectangular fin is the simplest among the plate fin surfaces. Heat exchanger surfaces with plain fins consist essentially of continuous passages of rectangular or trapezoidal cross section. Improvement of performance is caused primarily by the significant increase of secondary surface area. The average heat transfer coefficient also increases to some extent due to the developing flow over the entrance region. The heat transfer performance of a plain fin surface is generally poorer than that of more complex geometries such as the offset strip and the wavy fin surfaces at the same Reynolds number. But, because of its superior flow friction characteristics, a plain fin surface requires a smaller frontal area compared to other geometries for the same mass flow and heat transfer rates and pressure drop constraints. The required flow length, however, is higher for the same performance, leading to a greater overall volume.

2.1 The Plain Fin Geometry

The geometry of plain fin surface is defined by the following parameters:

(i) fin spacing (s), excluding the fin thickness,

(ii) fin height (h), excluding the fin thickness,

(iii) fin thickness (t), and

(iv) fin length (λ), in the flow direction

Figure 4.1 shows a schematic view of the plain fin surface of rectangular cross section and defines the geometric parameters. The following are some commonly used secondary parameters derived from the basic fin dimensions.

Frontal area (m^2) $A_F = (h + t)$ (per layer of unit width) (2.1)

Free flow area (m^2), $A_{ff} = \dfrac{sh}{s+t}$ (per layer of unit width) (2.2)

Free flow area to frontal area ratio $= \dfrac{sh}{(s+t)(h+t)}$ (2.3)

Primary heat transfer area density (m^2/m^3)

$$A_p''' = \frac{2s}{(s+t)(h+t)} \tag{2.4}$$

Secondary heat transfer area density (m^2/m^3)

$$A_s''' = \frac{2h}{(s+t)(h+t)} \tag{2.5}$$

Total heat transfer area density (m^2/m^3)

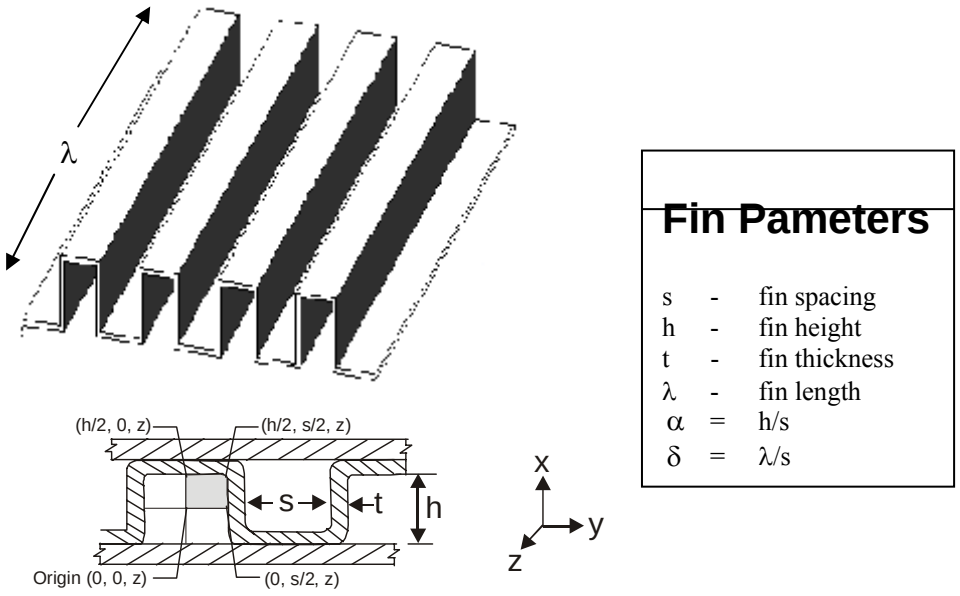

Figure 2.1: Geometry of a plain fin surface and the coordinate system for CFD analysis

$$A''' = A_p''' + A_s''' = \frac{2(s+h)}{(s+t)(h+t)} \tag{2.6}$$

Hydraulic diameter (m), $D_h = \frac{2sh}{s+h}$ (2.7)

Two dimensionless parameters: α = h/s and $\delta = \lambda/s$, have been identified for organizing heat transfer and flow friction data and for deriving correlations. Unlike that of interrupted fin geometries, the thermal performance of a plain fin surface depends little on the fin thickness t for given s and h. The small pressure drop, created by the sudden contraction and expansion of the flow cross section on entrance and exit respectively, is usually neglected.

The plain fin surface is often treated as a set of rectangular conduits in parallel and heat transfer correlations relevant to appropriate non-circular ducts are used for predicting performance. Because the passage length is never very large, the thermal performance is

dominated by entrance region effects. Therefore it has been felt necessary to model the rectangular plain fin passage by CFD and generate working correlations, instead of using those for fully developed flow in ducts. Classical authors like Kays and London [1], Wieting [2] and Joshi and Webb [3] have used the hydraulic diameter D_h as the characteristic dimension in expressing heat transfer and flow friction data. In order to bring the entrance region effects into better focus, later authors have introduced additional parameters. Muzychka and Yovanovich [88, 89] have expressed their correlation as a function of two geometric parameters, namely dimensionless duct length $z^+ \left(= \frac{z}{l \mathrm{Re}_l} \right)$ and aspect ratio α, whereas those of Shah [86] and Yilmaz [87] contain multiple parameters. Shah [86] and Yilmaz [87] have taken the hydraulic diameter as the characteristic length, while Muzychka and Yovanovich [88, 89] have used the square root of cross sectional area. In this analysis, we have used the hydraulic diameter D_h to define the Reynolds number. In addition, we have used the two dimensionless parameters h/s and λ/s to generate the heat transfer and flow friction correlations.

2.2 Computational Domain, Boundary conditions and the numerical model

Figure 2.2 shows the computational domain taken for modeling the flow passage. Considering the symmetry of the cross section, one fourth of the passage, cut along the two symmetry planes, is considered for CFD analysis. Half the fin height (h/2) in the x-direction, half the fin spacing (s/2) in the y-direction and the fin or passage length (□) in the z-direction constitute the computational domain. Figure 2.1 shows the coordinate system. The origin in the x, y plane is at the centre of the duct or the intersection of the two symmetry planes. Three-dimensional rectangular grids, shown in Fig 2.3, have been employed for meshing the system.

Boundary conditions

The boundaries of the computational domain consist of two solid surfaces (plate and fin) and two symmetry planes, is additions to the fluid inlet and exit planes. The boundary conditions are stated as follows.

- All solid (plate and fin) surfaces:

(i) [$x = h/2; 0 < y \le s/2; 0 < z \le \lambda$], and

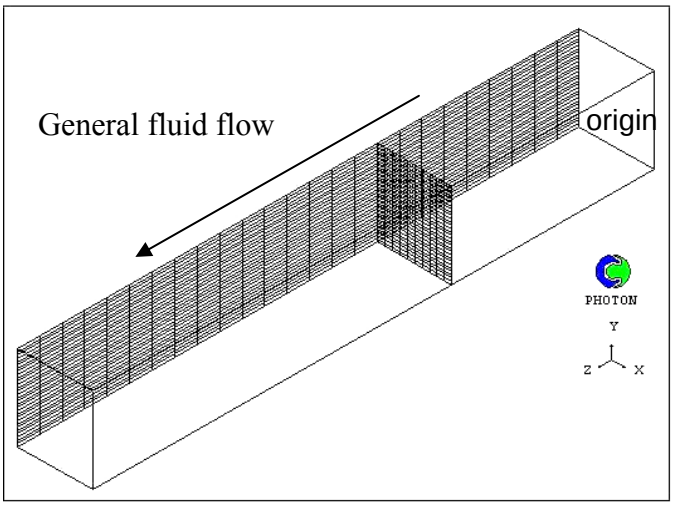

Figure 2.3: Computational grid for plain fins (laminar flow model)

(ii) [$0 < x \le h/2, y = s/2, 0 < z \le \lambda$]

No - slip and isothermal-boundary condition :

$$\left.\begin{aligned} u = v = w = 0 \\ T = T_w \end{aligned}\right\} \qquad (2.8)$$

- All no-solid-wall symmetry surfaces

(i) [$x = 0; 0 < y \le s/2; 0 < z \le \lambda$]

(ii) [$0 < x \le h/2, y = 0, 0 < z \le \lambda$]

Symmetry boundary condition :

$$\left.\begin{aligned} u = v = \frac{\partial w}{\partial x} = \frac{\partial w}{\partial y} = 0 \\ \frac{\partial T}{\partial x} = \frac{\partial T}{\partial y} = 0 \end{aligned}\right\} \qquad (2.9)$$

- Fluid inlet plane

(i) [$0 \le x \le h/2; 0 \le y \le s/2; z = 0$]

Uniform velocity :

$$\left.\begin{aligned} u = v = 0; w = w_0 \\ T = T_0 \end{aligned}\right\} \qquad (2.10)$$

- Fluid exit plane

$$[\ 0 < x \le h/2;\ 0 < y \le s/2;\ z = \lambda]$$

Fin Specifications

Fin pitch = 6.2 per in = 244.1 per m
Plate spacing, b = 0.405 in =10.29 x 10^{-3} m
Flow passage hydraulic diameter,
$4r_h$ = 0.0182 ft = 5.54 x 10^{-3} m
Fin metal thickness = 0.010 in,
aluminium = 0.254 x 10^{-3} m
Total transfer area/volume between plates,
β = 204 ft^2/ft^3 = 669.3 m^2/m^3

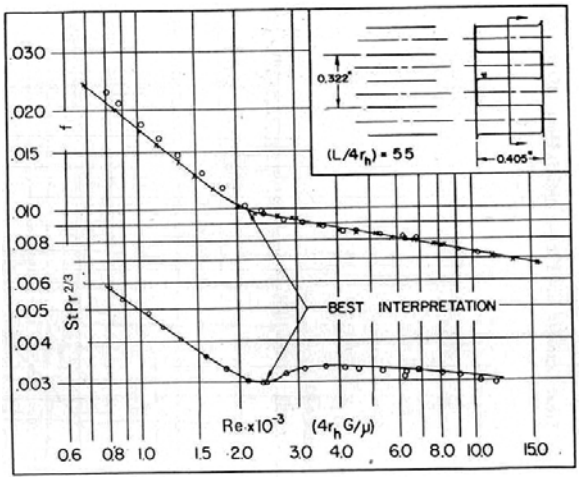

Figure 2.4 Plain fin surface (a) fin details (b) measured j and f data (Ref: Kays and London [1] Figure 10.24, Surface 6.2)

Constant pressure boundary condition:

$$p = 0 \qquad (2.11)$$

- Fully developed flow field

In case of sufficiently long ducts, the entrance region has a negligible effect on the overall thermo hydraulic performance of a surface. We have assumed fully developed velocity and temperature fields.

Procedures for calculating 'f' & 'j' for given Re, 'h/s' & 'λ/s'.

1. The mesh was first generated for identifications of Finite Volume Method in Gambit .It was then exported after specifying the relevant boundary conditions.
2. The specified geometry was read in fluent as case file and then GRID check was followed
3.Solver->viscous –laminar, activate energy equation, segregated.
4.Material selected was air
5.Operating conditions were default values

6.Boundary conditions.

- **Inlet conditions**

Temp of inlet(T_w)=300K.

Velocity at inlet v=(μ*R/D_h * ρ)

- **Outlet Conditions**

Back flow temperature=305K,p=0.

- **Wall Conditions**;

Temp pf wall=320K

Thickness of wall=.00254m

7. Solution; Under Relaxation factors

Values of pressure density, body forces, momentum and energy are provided continuously till the solution gets converged.

8. Discritizartion; pressure standard

Pressure velocity coupling Simple.

Momentum:-First Order Upwind

Energy;-First Order Upwind.

9.Monitors;-Residual:-Plot is selected.

10. Ieteration is carried until the values converge.

11. The difference of pressure from inlet and outlet is computated and 'j' and 'f' factors are calculated.

12. The mean temp. is calculated by writing the values of temp at exit and velocity at exit and applying formulae $T_m = \Sigma VT/\Sigma V$.

2.4 Computation of j and f factors

The friction factor **f** is computed from the area averaged mean pressure drop over the fin or passage length λ using the relation:

$$f = \frac{D_h \Delta p}{2\rho\lambda w_m^2} \tag{2.12}$$

which is derived from eq (1.2) by replacing the mass velocity G with ρw_m. In equation (4.12),

Δp = $p_m(0)-p_m(\lambda)$, $p_m(z)$ being the mean pressure over the cross section at axial coordinate z,

D_h = hydraulic diameter, and

w_m = area averaged mean velocity at any section.

The Colburn factor **j** defined in equation (1.1) can be rewritten in terms of the output variables of CFD simulation.

$$\mathbf{j} = \frac{D_h}{4\lambda} \mathrm{Pr}^{2/3} \ln\left(\frac{T_m(0) - T_w}{T_m(\lambda) - T_w}\right) \tag{2.13}$$

In equation (4.13) T_w is the wall temperature, assumed uniform around the computational domain. The mean variables w_m, $p_m(z)$ and $T_m(z)$ are computed from the following expressions.

Frontal area of section z, $A_F(z) = \iint dx \cdot dy$ (2.14)

Mean velocity, $w_m(z) = \frac{1}{A_F(z)} \iint w(x,y,z).dx \cdot dy$ (2.15)

Mean pressure, $p_m(z) = \frac{1}{A_F(z)} \iint p(x,y,z).dx \cdot dy$ (2.16)

Mean temperature, $T_m(z) = \frac{1}{A_F(z) w_m(z)} \iint T(x,y,z)\, w\,(x,y,z)\, dx \cdot dy$ (2.17)

All the double integrals in equations (2.14) – (2.17) are evaluated by summing over the available flow cross section at axial position z as shown in Fig. 2.2.

Table 1.1:Simulated values from CFD Software FLUENT 6.1

R	h/s	l/s	f	j
100	12	50	0.214	0.062
200	12	50	0.111	0.0334
500	12	50	0.0488	0.015
1000	12	50	0.0278	0.0085
2000	12	50	0.017	0.0049
5000	12	50	0.0096	0.0024
10000	12	50	0.0065	0.0016
100	12	10	0.2586	0.075
200	12	10	0.147	0.0411
500	12	10	0.0778	0.01999
1000	12	10	0.0507	0.0129
2000	12	10	0.034	0.0079
5000	12	10	0.0206	0.0046
10000	12	10	0.0144	0.0031
100	8	50	0.205	0.053
200	8	50	0.1065	0.0318
500	8	50	0.047	0.014
1000	8	50	0.027	0.0082
2000	8	50	0.0168	0.0045
5000	8	50	0.0095	0.0024
10000	8	50	0.0064	0.0015
100	8	10	0.242	0.07
200	8	10	0.143	0.038
500	8	10	0.081	0.0192
1000	8	10	0.05	0.0119
2000	8	10	0.0335	0.0077
3000	8	10	0.0231	0.006
5000	8	10	0.02	0.0045
6000	8	10	0.0182	0.004
8000	8	10	0.015	0.0034
10000	8	10	0.0139	0.00305
100	8	20	0.226	0.064
200	8	20	0.123	0.035
500	8	20	0.06	0.0162
1000	8	20	0.038	0.0096
2000	8	20	0.025	0.00599
5000	8	20	0.0143	0.0034
10000	8	20	0.01	0.0027
100	2	50	0.159	0.0326
200	2	50	0.083	0.0196
1000	2	50	0.0229	0.0053
2000	2	50	0.0145	0.0034
5000	2	50	0.0084	0.0019
10000	2	50	0.0057	0.0013
100	2	10	0.2037	0.0457
200	2	10	0.1147	0.027

500	2	10	0.0631	0.0145
1000	2	10	0.0419	0.0095
2000	2	10	0.0302	0.0064
5000	2	10	0.0185	0.0039
10000	2	10	0.013	0.0027

Graph 1.1

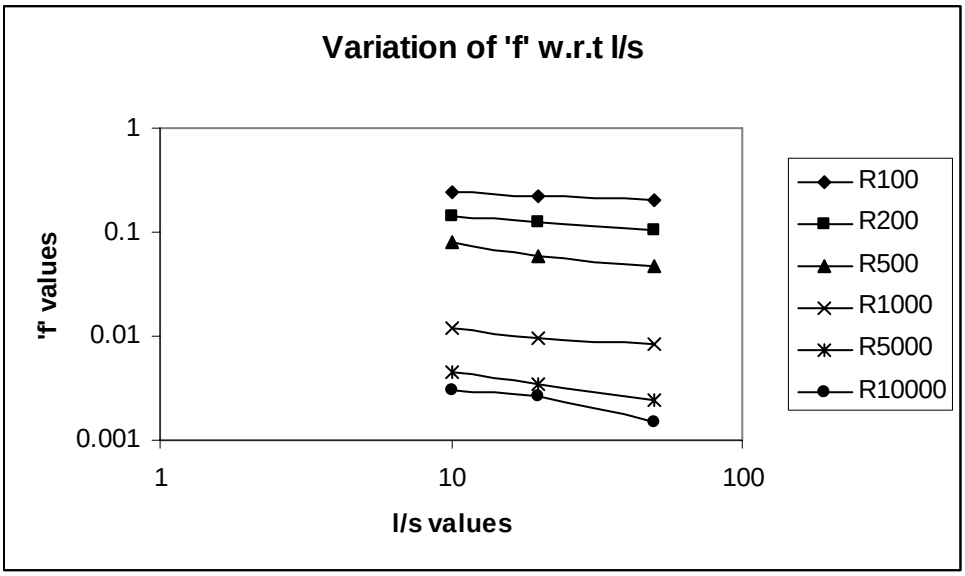

At h/s=12

Graph 1.2

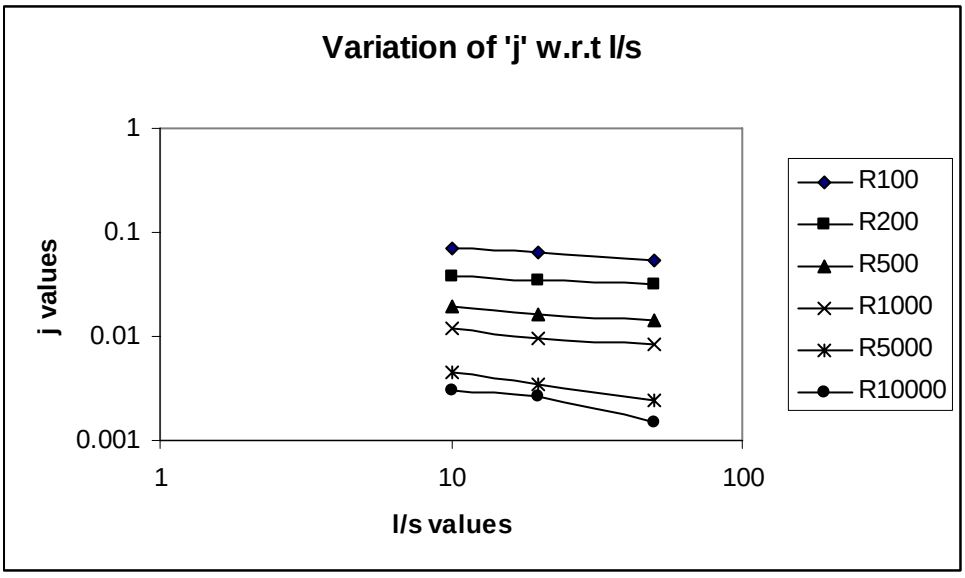

At h/s=12

Graph 1.3

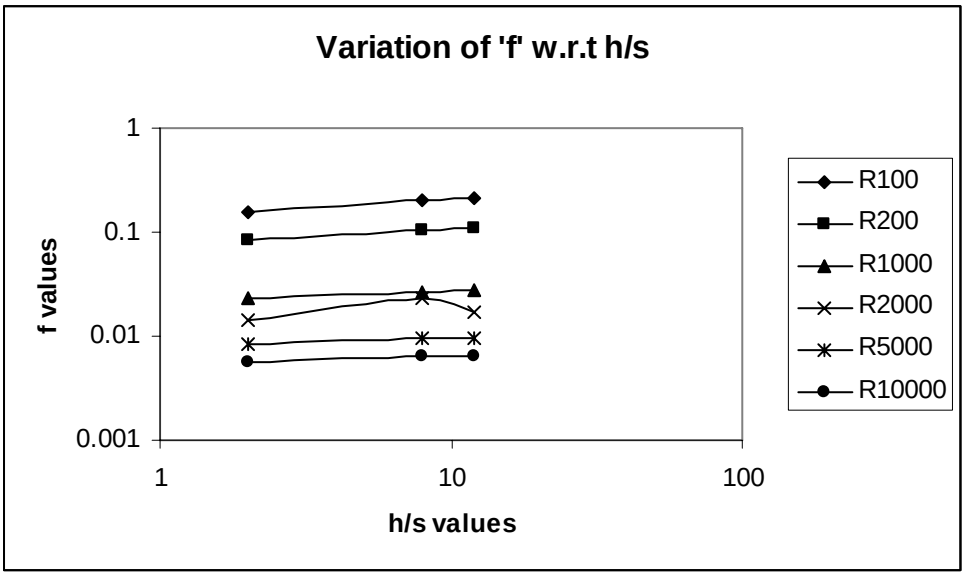

At l/s=10

Graph1.4

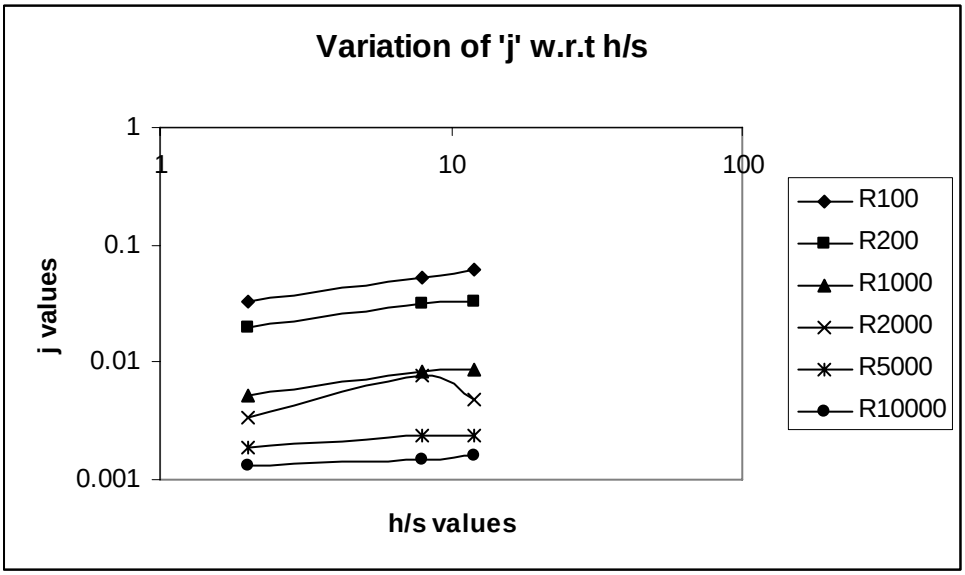

At h/s=12

Graph 1.5

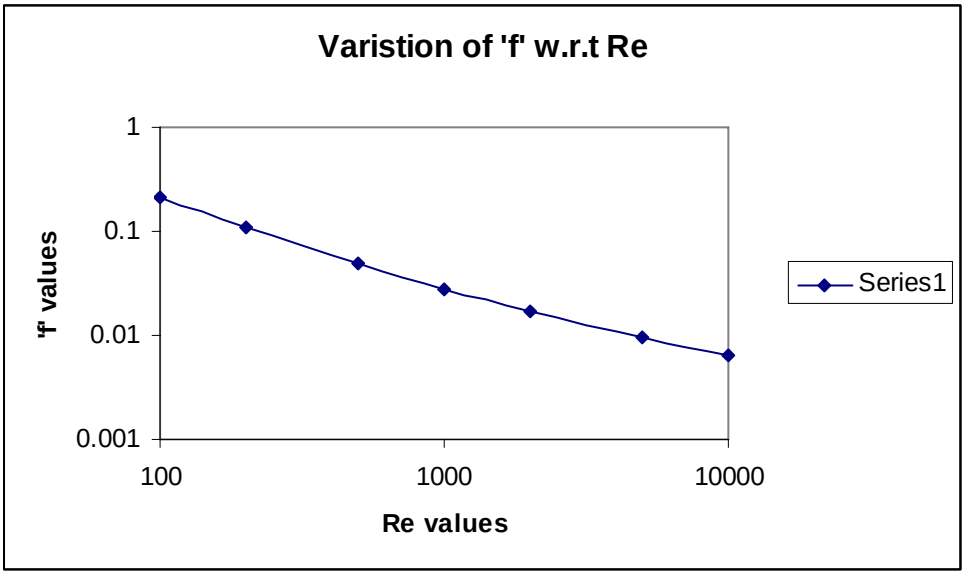

At h/s=12,l/s=50

Graph 1.6

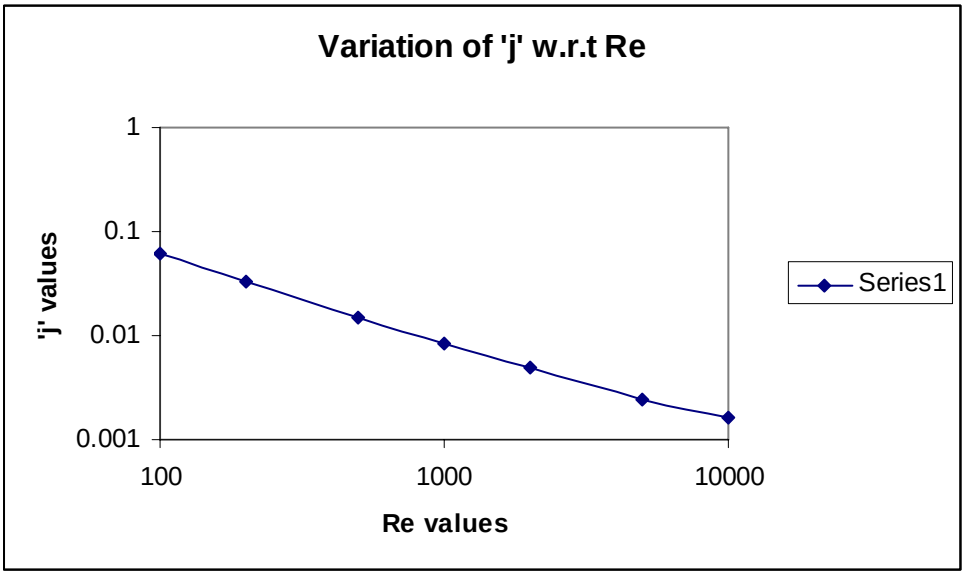

At h/s=12,l/s=50

Chapter 3

RECTANGULAR OFFSET STRIP FIN SURFACES

- The Offset Strip Fin Geometry
- Computational Domain, Boundary Conditions and Numerical Model
- Velocity and Temperature Fields
- Computation of **j** and **f** factors
- Role of Reynolds Number and Geometric parameters
- Generation of Hear Transfer and Flow Friction Correlations

The offset strip fin is one of the most widely used finned surfaces, particularly in high effectiveness heat exchangers employed in cryogenic and aircraft applications. These fins are created by cutting a set of plain rectangular fins periodically along the flow direction, and shifting each strip thus generated by half the fin spacing alternately left and rightward. The flow is thus periodically interrupted, leading to creation of fresh boundary layers and consequent heat transfer enhancement. Interruption of flow also leads to greater viscous pressure drop, manifested by a higher value of effective friction factor. In addition to the effect of wall shear, resistance to flow also increases due to *form drag* over the leading edges of the fin sections facing the flow, and due to trailing edge vortices. The effective heat transfer coefficient and friction factor are composite effects of the above mechanisms.

3.1 The Offset Strip Fin Geometry

The geometry of the offset strip fin surface is described by the following parameters:

(i) fin spacing (s), excluding the fin thickness,

(ii) fin height (h), excluding the fin thickness,

(iii) fin thickness (t), and

(iv) the strip length (□), in the flow direction.

The lateral fin offset is generally uniform and equal to half the fin spacing (including fin thickness). Figure 3.1 shows a schematic view of the rectangular offset strip fin surface and defines the geometric parameters. The following are some commonly used secondary parameters derived from the basic fin dimensions.

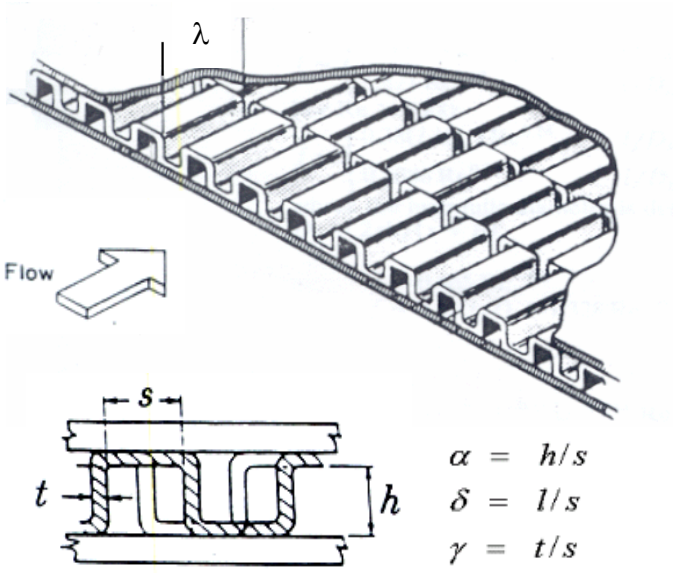

Fin Parameters

s	-	fin spacing
h	-	fin height
t	-	fin thickness
λ	-	strip length
α	=	h/s
δ	=	λ/s
γ	=	t/s

Figure 3.1: Geometry of a typical offset strip fin surface

Frontal area (m^2) $A_F = (h + t)$ (per layer of unit width) (3.1)

Free flow area (m^2), $A_{ff} = \dfrac{(s - t)h}{s + t}$ (per layer of unit width) (3.2)

Free flow area to frontal area ratio

$$= \frac{(s - t)h}{(s + t)(h + t)} \tag{3.3}$$

Primary heat transfer area density (m^2/m^3)

$$A_p''' = \frac{2s}{(s + t)(h + t)} \tag{3.4}$$

Secondary heat transfer area density (m^2/m^3)

$$A_s''' = \frac{2h(\lambda + t)}{(s + t)(h + t)\lambda} \tag{3.5}$$

Total heat transfer area density (m^2/m^3)

$$A''' = A_p''' + A_s''' = \frac{2(\lambda h + \lambda s + ht)}{(s + t)(h + t)\lambda} \tag{3.6}$$

Hydraulic diameter (m), $D_h = \dfrac{2(s - t)h\lambda}{\lambda h + \lambda s + ht}$ (3.7)

Fin volume per layer unit width = $\dfrac{t(h + s + t)}{s + t}$ (3.8)

These derived parameters are universally used in heat exchanger formulas and design procedures. In addition to these parameters, a set of dimensionless quantities have been defined, largely for expressing heat transfer and flow friction data and for deriving heat transfer correlations.

$$\left.\begin{aligned} \alpha &= h/s \\ \gamma &= t/s, \text{ and} \\ \delta &= \lambda/s \end{aligned}\right\} \tag{3.9}$$

The fin spacing s has been chosen as the reference dimension for all the three parameters. A review of current literature shows that a common and universally accepted set of such dimensionless quantities is yet to evolve. Weiting [2] has expressed his correlations in terms of dimensionless geometric parameters λ/D_h and s/h for Re<1000 and λ/D_h and t/D_h for Re>2000. Joshi and Webb [3] use λ/D_h, s/h and t/D_h as primary parameters in their

correlations with hydraulic diameter defined by eq (3.7). Manglik and Bergles [4], on the other hand, have used s/h, t/λ and t/s in their composite correlation for laminar, transition and turbulent regions, defining $D_h = \frac{4sh\lambda}{2(\lambda h + \lambda s + ht) + ts}$. Because in most practical cases, the hydraulic diameter D_h is strongly related to the fin spacing s, we feel that a single characteristic dimension is a more elegant choice.

3.2 Computational Domain, Boundary Conditions and the Numerical Model

Figure 3.2 shows the computational domain employed for modeling an offset strip fin surface in steady flow. The domain takes full advantage of the geometrical symmetries of the

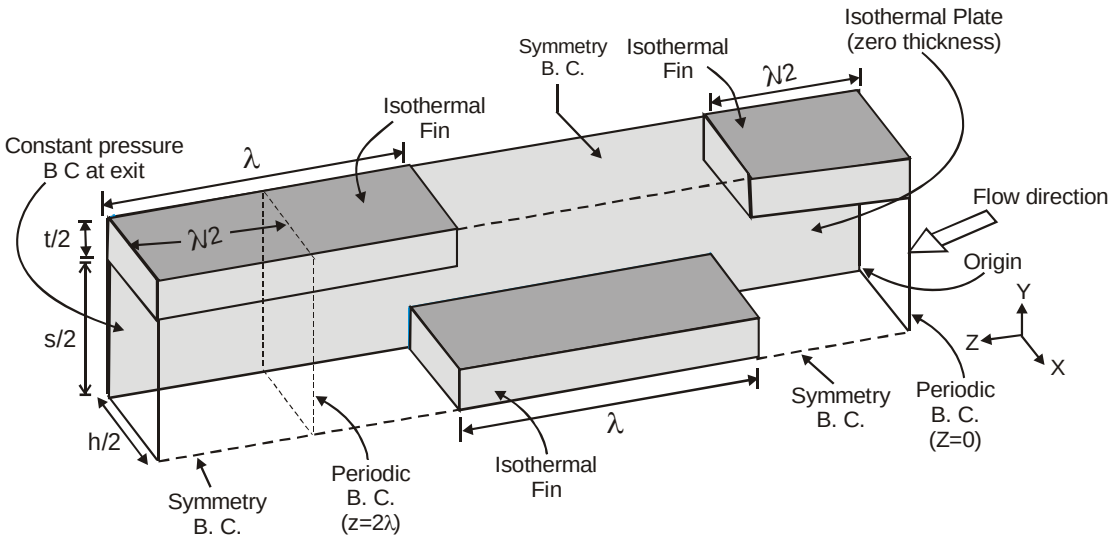

Figure 3.2: Computational domain with boundary conditions for offset strip fin surface

system. Half the fin height (h/2) in the x direction, half the fin spacing (s/2) in the y direction and two and half times the strip width (5λ/2) in the z direction constitute the computational domain. Three-dimensional rectangular grids, shown in Figure 3.3 have been employed for meshing the system.

Boundary conditions

- No-slip and isothermal boundary conditions:

$$\left.\begin{aligned} u = v = w = 0 \\ T = T_w \end{aligned}\right\} \qquad (3.10)$$

over all solid (plate and fin) surfaces and in interior of solid regions.

Plate surface: $x = 0;\ 0 < y \le (s+t)/2;\ 0 < z \le 5\square/2.$

Fin volume: $0 < x \le h/2;\ s/2 < y \le (s+t)/2;\ 0 < z \le \square/2.$

Fin volume: $0 < x \le h/2;\ 0 < y \le t/2;\ \lambda/2 < z \le 3\square/2.$

Fin volume: $0 < x \le h/2;\ s/2 < y \le (s+t)/2;\ 3\lambda/2 < z \le 5\square/2.$

The zero velocity and isothermal conditions are true not only on the solid surfaces but also in the interiors of the solid regions of the fins. Because the solid regions are counted inside the solution domain, the known conditions are stated accordingly.

- Symmetry boundary condition :

$$\left.\begin{aligned} u = v = \frac{\partial w}{\partial x} = \frac{\partial w}{\partial y} = 0 \\ \frac{\partial T}{\partial x} = \frac{\partial T}{\partial y} = 0 \end{aligned}\right\} \qquad (3.11)$$

over all no-solid-wall symmetric surfaces

$0 < x \le h/2,\ y = 0,\ 0 < z \le \lambda/2;$

$0 < x \le h/2,\ y = (s+t)/2,\ \lambda/2 < z \le 3\lambda/2;$

$0 < x \le h/2,\ y = 0,\ 3\lambda/2 < z \le 5\lambda/2;$

$x = h/2,\ 0 < y \le (s+t)/2,\ 0 < z \le 5\lambda/2;$

- Fluid Entrance Plane:

  The simulation has been carried out for the (globally) fully developed flow, with periodic velocity and temperature fields established. This periodicity condition is stated as:

$$\left.\begin{aligned} u(x, y, 2\lambda) &= u(x, y, 0) \\ v(x, y, 2\lambda) &= v(x, y, 0) \\ w(x, y, 2\lambda) &= w(x, y, 0) \\ p(x, y, 2\lambda) &= p(x, y, 0) - \Delta p \\ \theta(x, y, 2\lambda) &= \theta(x, y, 0) \end{aligned}\right\} \quad (3.12)$$

  The dimensionless temperature θ is defined as:

$$\theta(x, y, z) = \frac{T(x, y, z) - T_w}{T_b(z) - T_w} \quad (3.13)$$

  $T_b(z)$ being the mean bulk temperature at axial position z.

- Total flow rate at inlet : [$0 < x \le h/2$; $0 < y \le s/2$; $z = 0$]

$$\int_{x=0}^{h/2} \int_{y=0}^{s/2} \rho w \, dx \, dy = Ghs/4, \quad (3.14)$$

  G being the specified average mass velocity at inlet. The total flow rate condition replaces the required velocity boundary conditions.

- Bulk temperature of fluid at inlet: [$0 < x \le h/2$; $0 < y \le s/2$; $z = 0$]

$$T_b(z=0) = T_0 \quad (3.15)$$

- Exit plane: [$0 < x \le h/2$; $0 < y \le s/2$; $z = 5\lambda/2$]

  Constant pressure boundary condition:

$$p = 0$$

3.4 Computation of j and f Factors

The friction factor **f** is computed from the area averaged mean pressure drop over the periodic length 2□ using the relation:

$$\mathbf{f} = \frac{D_h \Delta p}{4\rho\lambda w_{mf}^2} \tag{3.17}$$

where,

$\Delta p = p_m(0) - p_m(2\lambda)$, $p_m(z)$ being the mean pressure over the cross section at z,

D_h = hydraulic diameter, and

w_{mf} = area averaged mean velocity at the minimum free flow section.

The Colburn factor **j** defined in eq (1.1) can be rewritten in terms of the output variables of CFD simulation.

$$\mathbf{j} = \frac{D_h}{8\lambda} \mathrm{Pr}^{2/3} \ln\left(\frac{T_m(0) - T_w}{T_m(\lambda) - T_w}\right) \tag{3.18}$$

In equation (3.18), T_w is the wall temperature assumed uniform around the computational domain. The mean variables w_m, $p_m(z)$ and $T_m(z)$ are computed from the following expressions.

Frontal area of section z, $A_F(z) = \iint dx \cdot dy$ (3.19)

Mean velocity, $w_m(z) = \frac{1}{A_F(z)} \int\int w(x,y,z).dx \cdot dy$ (3.20)

Mean pressure, $p_m(z) = \frac{1}{A_F(z)} \int\int p(x,y,z).dx \cdot dy$ (3.21)

Mean temperature, $T_m(z) = \frac{1}{A_F(z) w_m(z)} \iint T(x,y,z)\ w\ (x,y,z)\ dx \cdot dy$ (3.22)

All the double integrals in equations (3.19 – 3.22) are evaluated by summing over the available flow cross section at axial position z as shown in Fig 3.2.

Table3.1 ‘f’ and ‘j’ obtained from simulation using FLUENT 6.1

Re	h/s	l/s	t/s	f	j
100	12	4	0.2	0.1313	0.0412
200	12	4	0.2	0.0807	0.0356
500	12	4	0.2	0.0613	0.03145
1000	12	4	0.2	0.0271	0.0195
5000	12	4	0.2	0.0121	0.0078
10000	12	4	0.2	0.0094	0.0063
100	12	4	0.05	0.1649	0.05411
200	12	4	0.05	0.1288	0.0461
500	12	4	0.05	0.0725	0.04298
1000	12	4	0.05	0.0384	0.0333
5000	12	4	0.05	0.0177	0.0203
10000	12	4	0.05	0.0132	0.01103
100	12	4	0.1	0.1547	0.0486
200	12	4	0.1	0.0949	0.0447
500	12	4	0.1	0.0683	0.04112
1000	12	4	0.1	0.0315	0.02748
5000	12	4	0.1	0.014	0.01013
10000	12	4	0.1	0.01002	0.0079
100	8	4	0.1	0.1312	0.041
200	8	4	0.1	0.0749	0.0395
500	8	4	0.1	0.0382	0.0335
1000	8	4	0.1	0.0242	0.01987
5000	8	4	0.1	0.0103	0.01004
10000	8	4	0.1	0.0086	0.0074
100	4	4	0.1	0.1161	0.032
200	4	4	0.1	0.0676	0.0286
500	4	4	0.1	0.0345	0.0246
1000	4	4	0.1	0.0222	0.0167
5000	4	4	0.1	0.0092	0.0096
10000	4	4	0.1	0.0069	0.0069
100	4	8	0.1	0.1063	0.0311
200	4	8	0.1	0.0596	0.0258
500	4	8	0.1	0.0282	0.0235
1000	4	8	0.1	0.0165	0.0154
5000	4	8	0.1	0.0057	0.0061
10000	4	8	0.1	0.0032	0.0046
100	4	12	0.1	0.1033	0.0281
200	4	12	0.1	0.0529	0.02476
500	4	12	0.1	0.0253	0.02109
1000	4	12	0.1	0.0142	0.0136
5000	4	12	0.1	0.0044	0.0033
10000	4	12	0.1	0.0029	0.0028

Graph 3.1

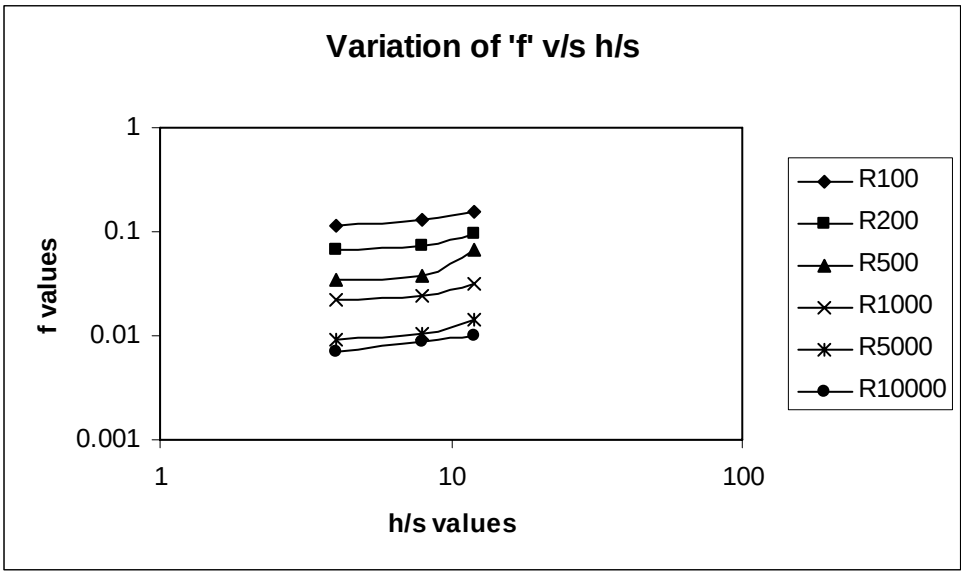

At l/s=4,t/s=.1

Graph 3.2

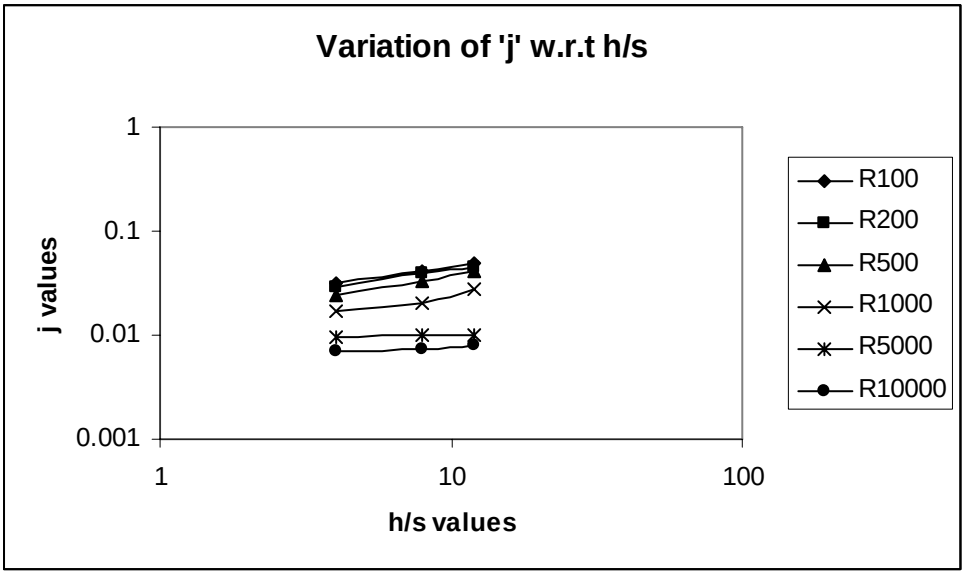

At l/s=4,t/s=.1

Graph 3.3

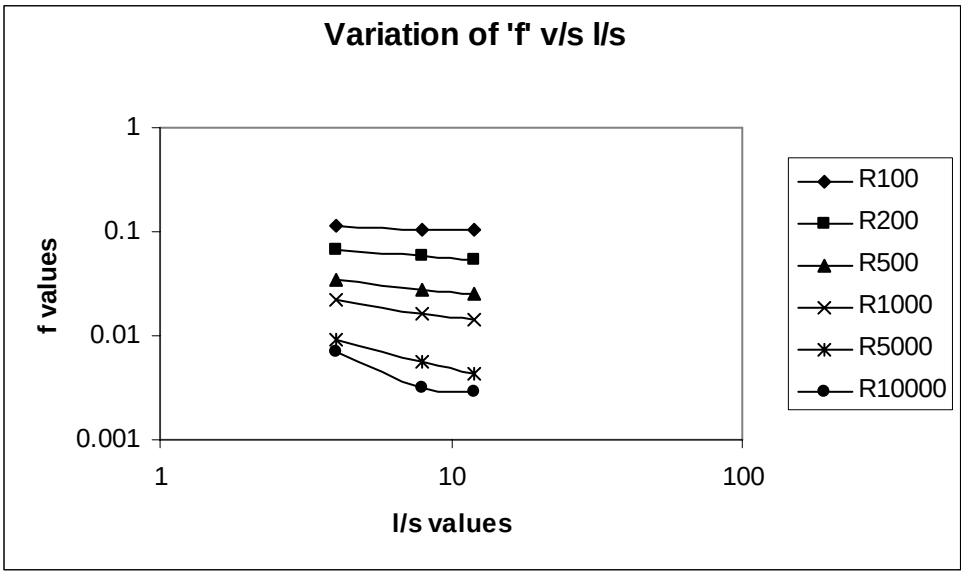

At h/s=4,t/s=.1

Graph 3.4

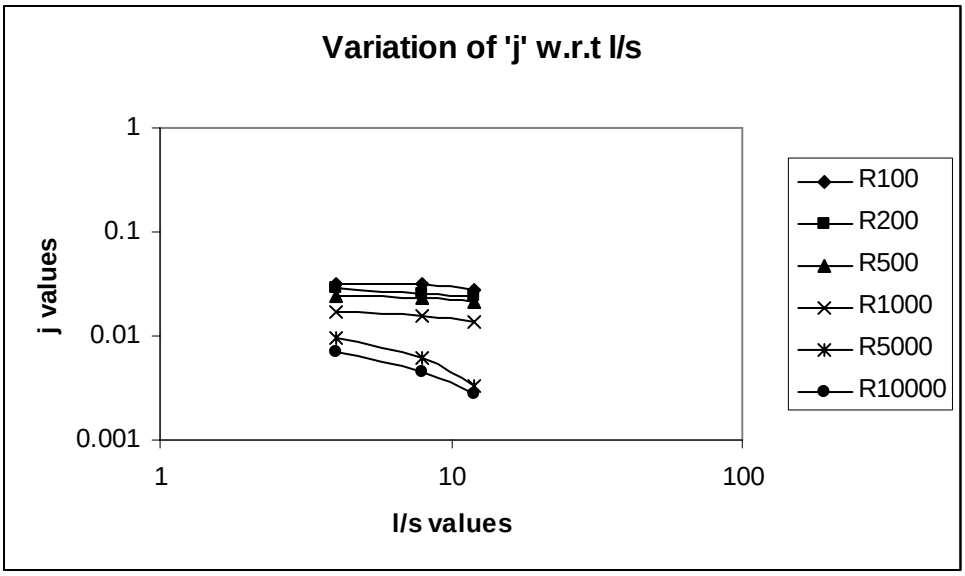

At h/s=4,t/s=.1

Graph 3.5

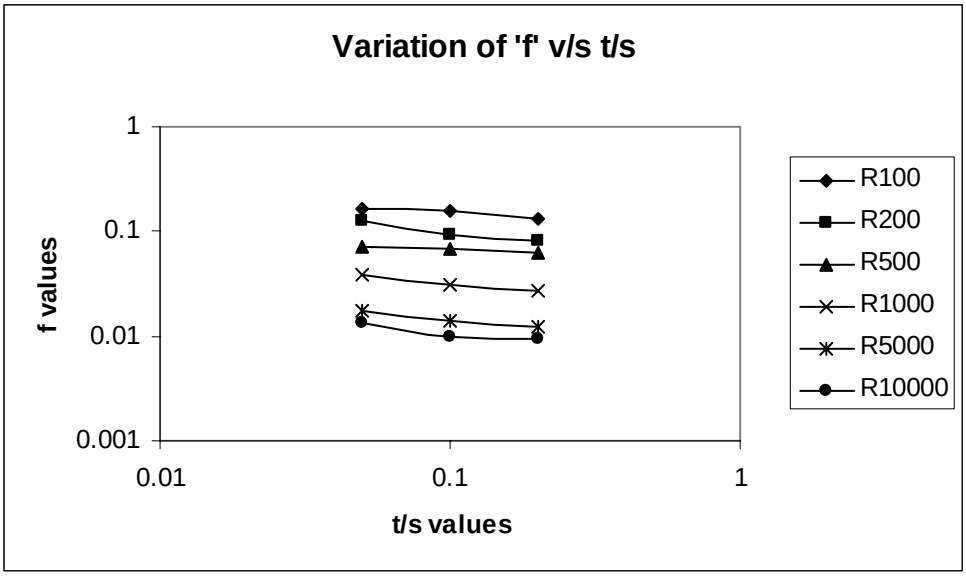

At h/s=12,t/s=4

Graph 3.6

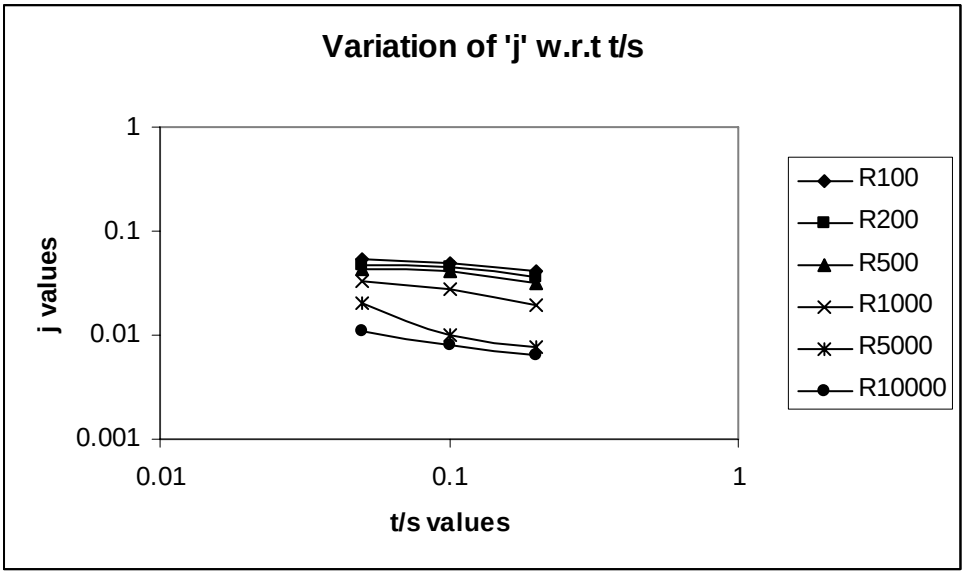

At h/s=12,t/s=4

Graph 3.7

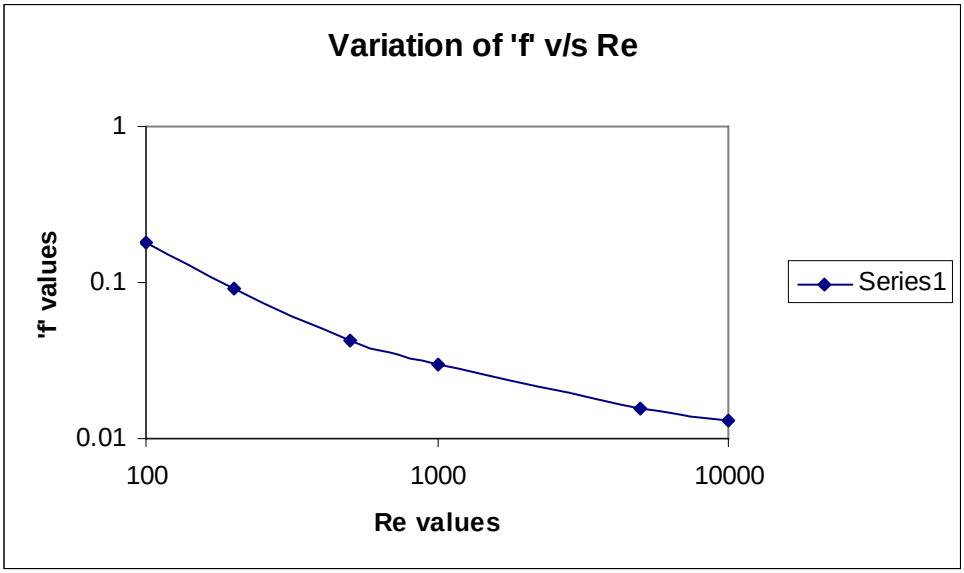

At h/s=4,l/s=8,t/s=.1

Graph 3.8

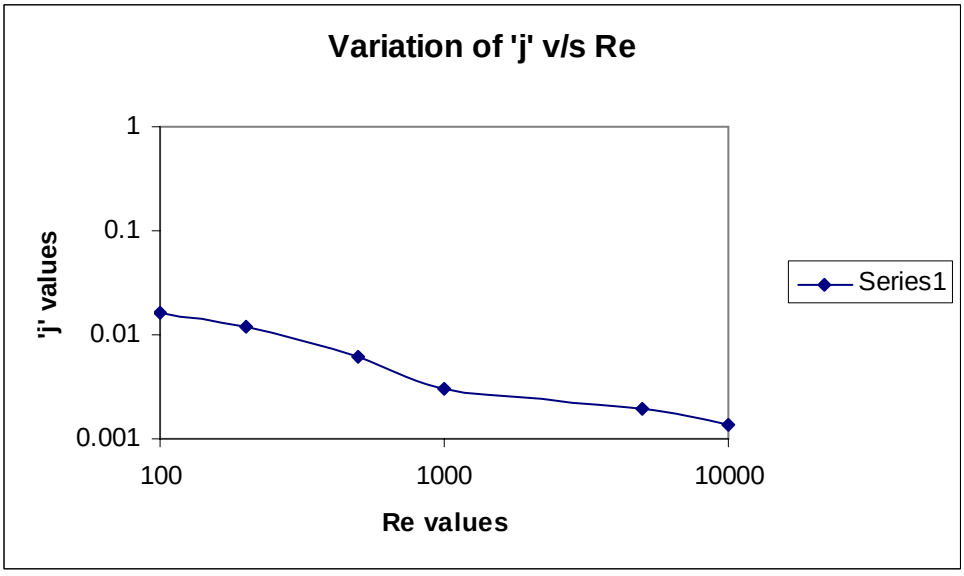

At h/s=4,l/s=8,t/s=.1

It is intended to express these results in the form of simple correlations that will prove to be convenient tools in practical heat exchanger design. It is proposed to seek the correlations in the form:

$$f \text{ or } j = C(\mathrm{Re})^{a0} \left(\frac{h}{s}\right)^{a1} \left(\frac{l}{s}\right)^{a2} \left(\frac{t}{s}\right)^{a3} \qquad (3.23)$$

The following procedure has been adopted for determining the indices C, a0-a3 of the correlations. Two separate sets of indices are necessary to express the f and j data. It is shown later in this section that the j and f vs Re data exhibit significant non-linearity over the Re range 100<Re<10,000. We have, therefore, expressed the correlations through two separate equations over the low and the high Re regimes. The following procedure is employed to arrive at the correlations.

Table 3.2: Determination of indices a1, a2 and a3 of heat transfer and flow friction correlation from single factor numerical experiments.

Friction factor f				Colburn factor j			
Re	***a1***	***a2***	***a3***	***Re***	***a1***	***a2***	***a3***
100	0.1764	-0.1272	-0.1644	100	0.2715	-0.2719	-0.06
200	0.1479	-0.1817	-0.095	200	0.2701	-0.2847	-0.069
500	0.1469	-0.2909	-0.064	500	0.2836	-0.2354	-0.075
1000	0.1244	-0.4281	-0.032	1000	0.2894	-0.1871	-0.065
5000	0.1629	-0.6907	-0.019	5000	0.2831	-0.1736	-0.039
10000	0.3177	-1.1085	-0.017	10000	0.2774	-0.1645	-0.033

Determination of indices a1-a3 from single factor (numerical) experiments

The data of Table 3.2 are analyzed in selected groups where all parameters except one (h/s, λ/s or t/s) are kept common at their average values. The data are plotted against the varying parameter in log-log scale and the slope determined. Table 3.2 gives the a1-a3 values for both f and j factors for several values of Re. The other two parameters are kept constant. It is observed that the indices determined from single factor experiments vary within small margins, over the Re ranges 0-1000 and 1000-10,000 separately. This observation justifies the power law assumption made in eq (3.23).

Chapter 4

WAVY FIN SURFACES

- The Wavy Fin Geometry
- Computational Domain, Boundary Conditions and Numerical Model
- Velocity and Temperature Fields
- Computation of **j** and **f** factors
- Role of Reynolds Number and Geometric parameters
- Generation of Heat Transfer and Flow Friction Correlations.

The wavy fin is one of the most popular fin types in plate fin heat exchangers, particularly where superior heat transfer performance is demanded under tight pressure drop allowance. The wavy geometry lengthens the flow path, creates turbulence and promotes better mixing. They are uninterrupted surfaces with cross-sectional shape similar to that of plain fins except for the undulations in the flow direction. The heat transfer and flow friction performance of wavy fin surfaces lies between those of plain and offset strip fins. Wavy fins are common in hydrocarbon industry where exchangers must cope with high mass velocities and moderate thermal duties. In aircraft applications, it is the preferred fin type on the ram air side, where available pressure drop allowance is rather small.

4.1 The Wavy Fin Geometry

There are two basic variants of the wavy fin geometry: the herringbone wave and the smooth wave. In the herringbone type, fins have plain angular bends while the smooth type has fins of sinusoidal shape. The geometry of the wavy fin is defined by the following parameters :

(i) fin spacing (s), excluding the fin thickness,
(ii) fin height (h), excluding the fin thickness
(iii) fin thickness (t),
(iv) projected fin length or wave length (Λ), and
(v) the wave amplitude (a)

Figure 4.1 shows a schematic view of the smooth wavy fin surface and defines the geometric parameters. The following set of dimensionless parameters is defined for the wavy fin, largely for expressing heat transfer and flow friction data and for deriving correlations.

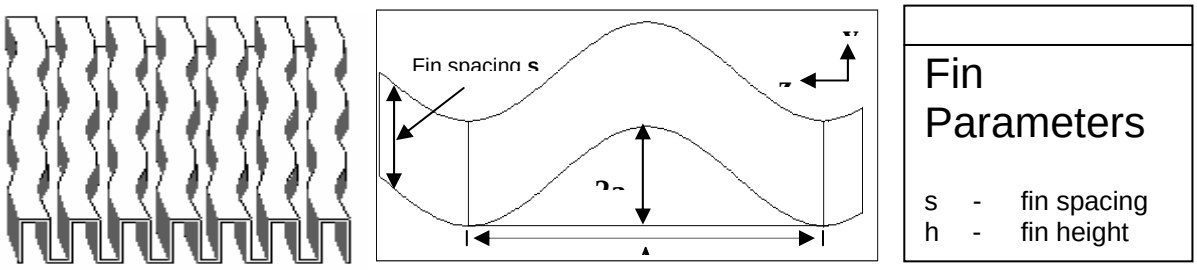

Figure 4.1: Geometry of a typical smooth wavy fin surface

$$\alpha = h/s$$
$$\beta = a/s, \text{ and}$$
$$\xi = \Lambda/a$$

Like other continuous fin types, the fin thickness in a wavy fin passage plays no role in core pressure drop. The heat transfer performance, however, improves with greater fin thickness through enhancement of fin efficiency. In this work, the effect of fin inefficiency has been neglected in evaluating heat transfer performance. Therefore, the fin thickness (t) is not a relevant parameter. Kim *et al* [164] and Wang *et al* [82, 83] have developed heat transfer and flow friction correlations for wavy–fin–and–tube heat exchangers with different sets of dimensionless geometric parameters. But no such correlations are available in open literature for wavy fin surfaces used in plate fin heat exchangers.

4.2Computational Domain, Boundary Conditions And the Numerical Model

Figure 4.2 shows the computational domain taken for modeling fluid flow and heat transfer over a smooth wavy surface. The advantage of geometrical symmetry along the fin height has been exploited in working out the extent of the computational domain. Half the fin height (h/2) in the x-direction, fin spacing (s) in the y-

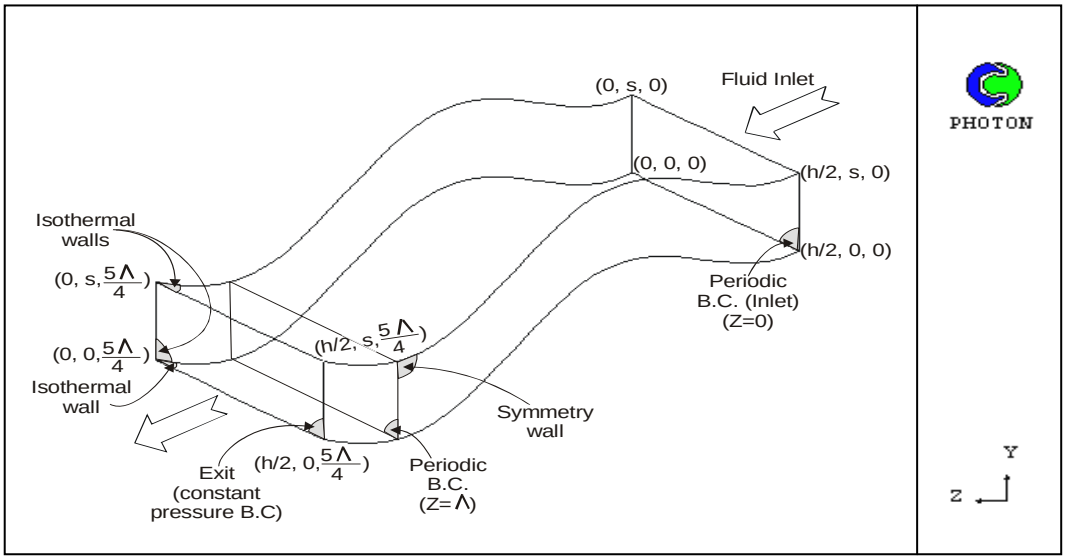

Figure 4.2: Computational domain with boundary conditions for smooth wavy fin surface

direction and a projected length of 5Λ/4 in the z-direction constitute the computational domain. The duct is thus made of two parallel flat surfaces normal the x direction and two parallel wavy surfaces perpendicular to it. Body-fitted coordinate system has been employed for modeling of both herringbone and smooth wavy fin passages. This coordinate system is ideally suited to modeling of complex geometries. The contours of the wavy surface are effectively represented by aligning the grid lines with the curved boundary walls. The lines bounding the two flat surfaces are described in terms of the wave amplitude a and the wavelength **Λ** by the equations: y = a(1-cos(2πz/Λ) and $y = s + a\left(1 - \cos\left(2\pi z/\Lambda\right)\right)$. The two wavy surfaces are separated by a distance s along the **y** direction, while the two flat surfaces are separated in the **x** direction by the fin height **h**. A body-fitted coordinate (BFC) grid is defined via the corner points where the cell faces intersect. These corner points are specified by their Cartesian coordinates

Boundary conditions

- No slip and isothermal condition

$$\left.\begin{aligned} u = v = w = 0 \\ T = T_w \end{aligned}\right\} \qquad (4.1)$$

over all solid (plate and fin) surfaces:

Plate surface: x = 0, 0 < y ≤ s, 0 < z ≤ 5Λ/4 ;

Fin surface: 0 < x ≤ h/2, y = 0, 0 < z ≤ 5Λ/4 ;

Fin surface: 0 < x ≤ h/2, y = s, 0 < z ≤ 5Λ/4.

- Symmetry boundary condition :

$$\left.\begin{aligned} u = v = \frac{\partial w}{\partial x} = \frac{\partial w}{\partial y} = 0 \\ \frac{\partial T}{\partial x} = \frac{\partial T}{\partial y} = 0 \end{aligned}\right\} \qquad (4.2)$$

over the no-solid-wall symmetric surface :

x = h/2, 0 < y ≤ s, 0 < z ≤ 5Λ/4 .

- Periodicity condition

$$\left.\begin{aligned} u(x, y, \Lambda) &= u(x, y, 0) \\ v(x, y, \Lambda) &= v(x, y, 0) \\ w(x, y, \Lambda) &= w(x, y, 0) \\ p(x, y, \Lambda) &= p(x, y, 0) - \Delta p \\ \theta(x,y, \Lambda) &= \theta(x,y,0) \end{aligned}\right\} \qquad (4.3)$$

over the periodic planes:

$0 < x \le h/2,\ 0 < y \le s,\ z = 0$ and

$0 < x \le h/2,\ 0 < y \le s,\ z = \Lambda$.

The dimensionless temperature θ is defined as:

$$\theta(x,y,z) = \frac{T(x,y,z) - T_w}{T_b(z) - T_w} \qquad (4.4)$$

$T_b(z)$ being the mean bulk temperature at axial position z.

- Total flow rate at inlet [$0 < x \le h/2,\ 0 < y \le s,\ z = 0$]

$$\int_{x=0}^{h/2} \int_{y=0}^{s} \rho\, w\, dx\, dy = \frac{Ghs}{2} \qquad (4.5)$$

G being the specified average mass velocity at inlet. The total flow rate condition replaces the required velocity boundary conditions.

- Bulk temperature of fluid at inlet : [$0 < x \le h/2,\ 0 < y \le s,\ z = 0$]

$T_b(z=0) = T_0$

- Constant pressure boundary condition :

$$p = 0 \qquad (4.6)$$

over the exit plane :

$0 < x \le h/2,\ 0 < y \le s,\ z = 5\Lambda/4$

4.3 Computation of j and f factors

Like in chapters 2 and 3, the friction factor **f** is computed from the area averaged mean pressure drop over the periodic length Λ using the relation:

$$f = \frac{D_h \Delta p}{2\rho \Lambda w_{mf}^2} \tag{4.7}$$

where, $\Delta p = p_m(0) - p_m(\Lambda)$,

D_h = hydraulic diameter, and

w_{mf} = area averaged mean velocity over any cross section.

The Colburn factor **j** is computed from the log mean temperature difference between the inlet and the exit sections, separated by a distance Λ.

$$\boldsymbol{j} = \frac{D_h}{4\Lambda} \cdot \mathrm{Pr}^{2/3} \ln\left(\frac{T_w - T_{m(0)}}{T_w - T_{m(\Lambda)}}\right) \tag{4.8}$$

T_w being the wall temperature, uniform around the computational domain. The area averaged mean variables are computed from the following expressions

Frontal area of section z, $A_F(z) = \iint dx \cdot dy$ (4.9)

Mean velocity, $w_m(z) = \frac{1}{A_F(z)} \iint w(x,y,z).dx \cdot dy$ (4.10)

Mean pressure, $p_m(z) = \frac{1}{A_F(z)} \iint p(x,y,z).dx \cdot dy$ (4.11)

Mean temperature, $T_m(z) = \frac{1}{A_F(z) w_m(z)} \iint T(x,y,z)\ w\ (x,y,z)\ dx \cdot dy$ (4.12)

Table 4.1 Values of ‘f’ and ‘j’ obtained from Simulation by FLUENT 6.1

Re	h/s	a/s	l/a	f	j
100	2	0.5	16	0.1152	0.01627
200	2	0.5	16	0.06902	0.01057
500	2	0.5	16	0.0408	0.005926
1000	2	0.5	16	0.0339	0.00288
5000	2	0.5	16	0.02	0.001803
10000	2	0.5	16	0.0169	0.001704
100	8	0.5	16	0.182	0.02417
200	8	0.5	16	0.0961	0.0123
500	8	0.5	16	0.0473	0.0067
1000	8	0.5	16	0.0342	0.00326
5000	8	0.5	16	0.022	0.00201
10000	8	0.5	16	0.0194	0.00176
100	12	0.5	16	0.19002	0.02558
200	12	0.5	16	0.1003	0.01572
500	12	0.5	16	0.04896	0.00718
1000	12	0.5	16	0.0348	0.00367
5000	12	0.5	16	0.02204	0.00234
10000	12	0.5	16	0.020067	0.0021
100	8	0.25	16	0.1829	0.02959
200	8	0.25	16	0.10331	0.01672
500	8	0.25	16	0.05763	0.00733
1000	8	0.25	16	0.04214	0.003566
5000	8	0.25	16	0.02748	0.00298
10000	8	0.25	16	0.02345	0.00219
100	8	1	16	0.17995	0.0165
200	8	1	16	0.092563	0.01203
500	8	1	16	0.04193	0.00602
1000	8	1	16	0.02979	0.003004
5000	8	1	16	0.01552	0.00192
10000	8	1	16	0.01316	0.00139
100	8	1	8	0.4021	0.07896
200	8	1	8	0.2463	0.04171
500	8	1	8	0.1473	0.0183
1000	8	1	8	0.1099	0.00969
5000	8	1	8	0.0893	0.0033
10000	8	1	8	0.0568	0.0021
100	8	1	4	0.7063	0.1087
200	8	1	4	0.3864	0.06428
500	8	1	4	0.3271	0.0284
1000	8	1	4	0.2584	0.0157
5000	8	1	4	0.1746	0.0061
10000	8	1	4	0.0972	0.0035

Graph 4.1

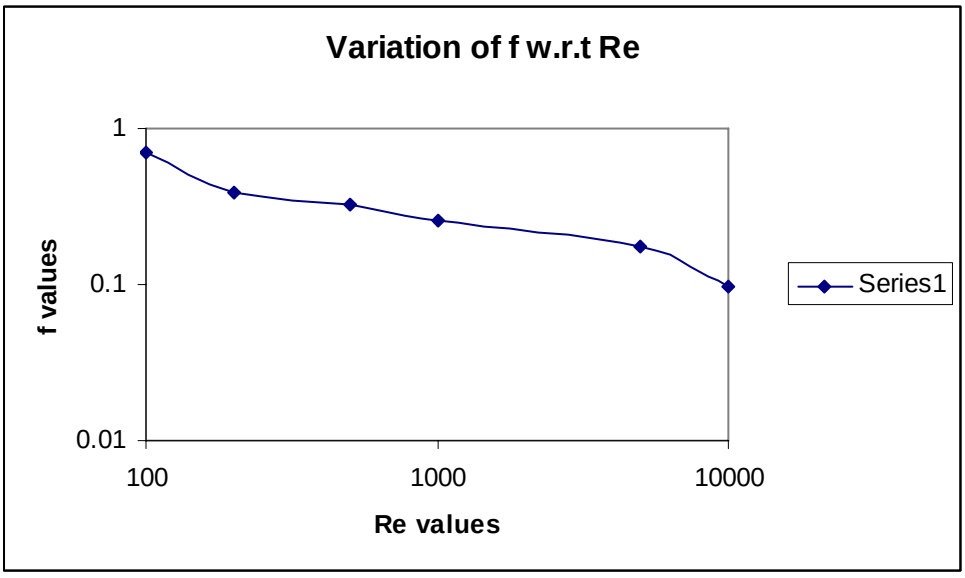

At h/s =8,l/a=16,a/s=1

Graph 4.2

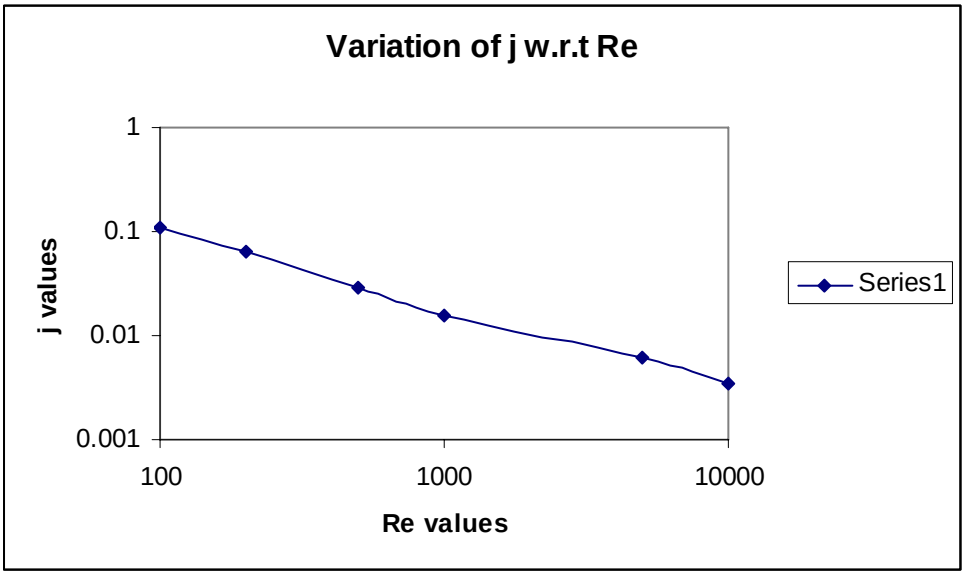

At a/s=.5 , l/s =16

Graph 4.3

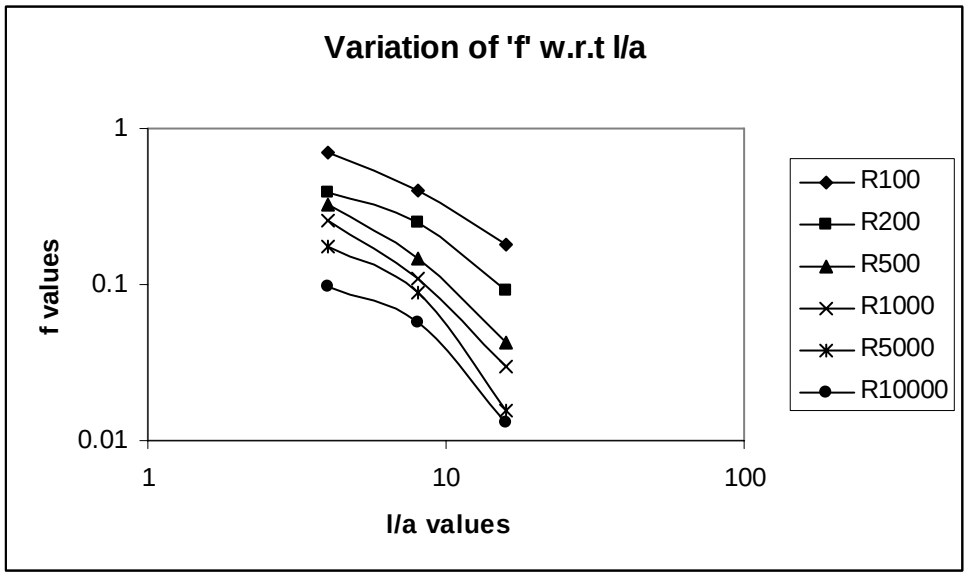

At h/s=8,a/s=1

Graph 4.4

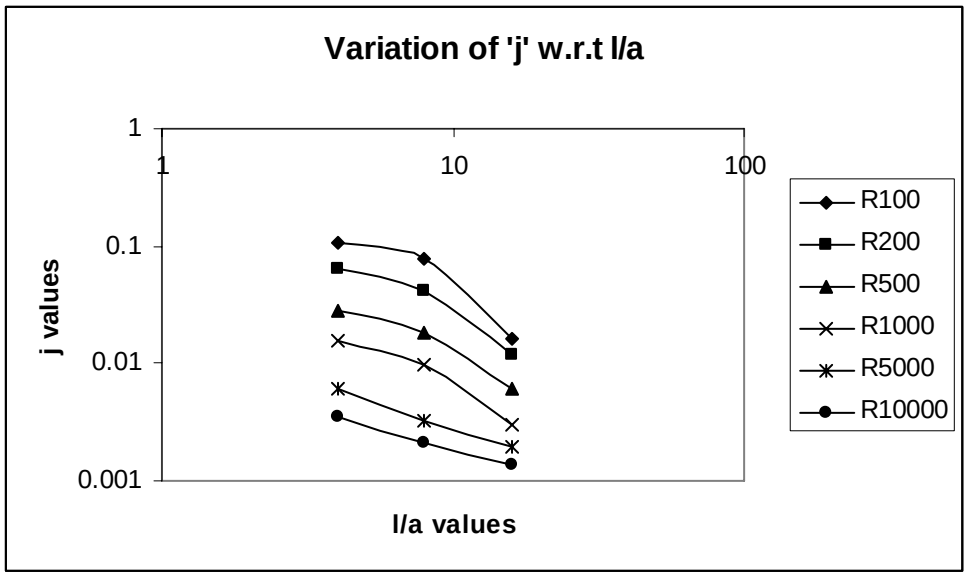

At h/s=8,a/s=1

Graph 4.5

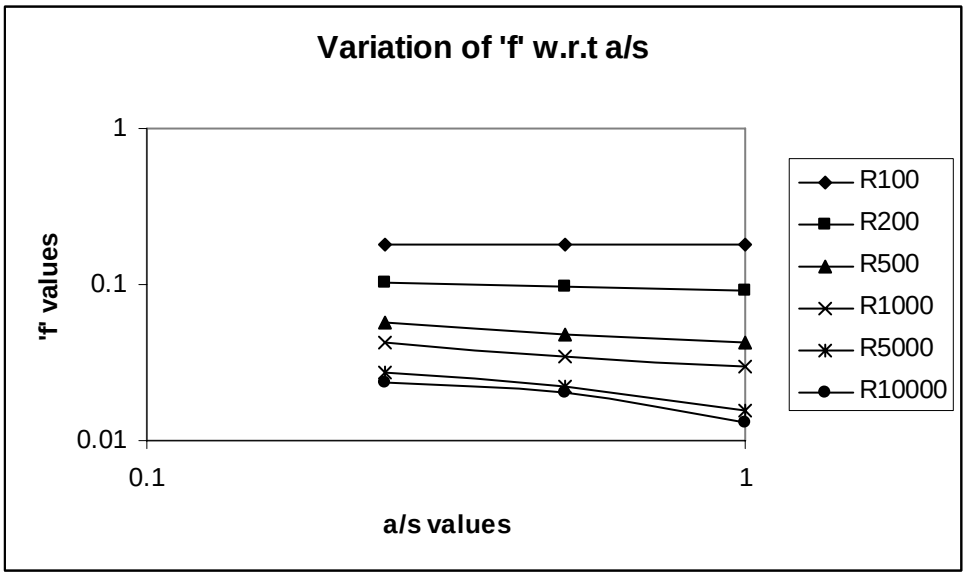

At h/s=8,l/s=16

Graph 4.6

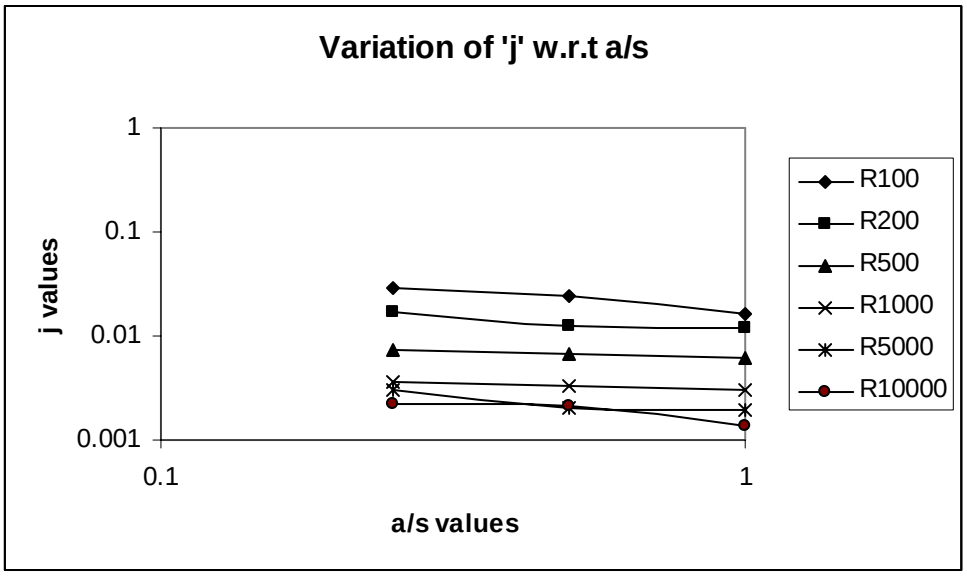

At h/s=8,l/s=16

Graph 4.7

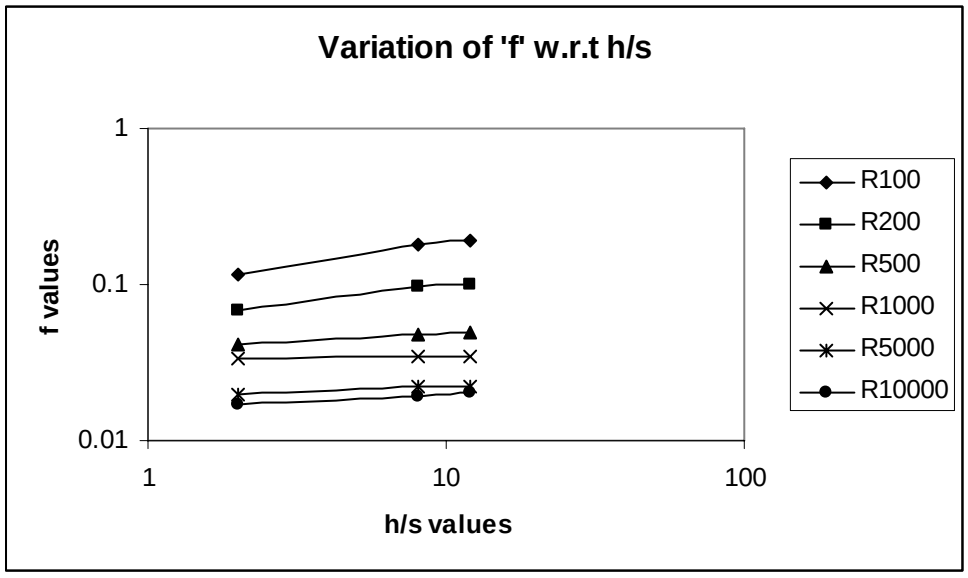

At a/s=.5 , l/s =16

Graph 4.8

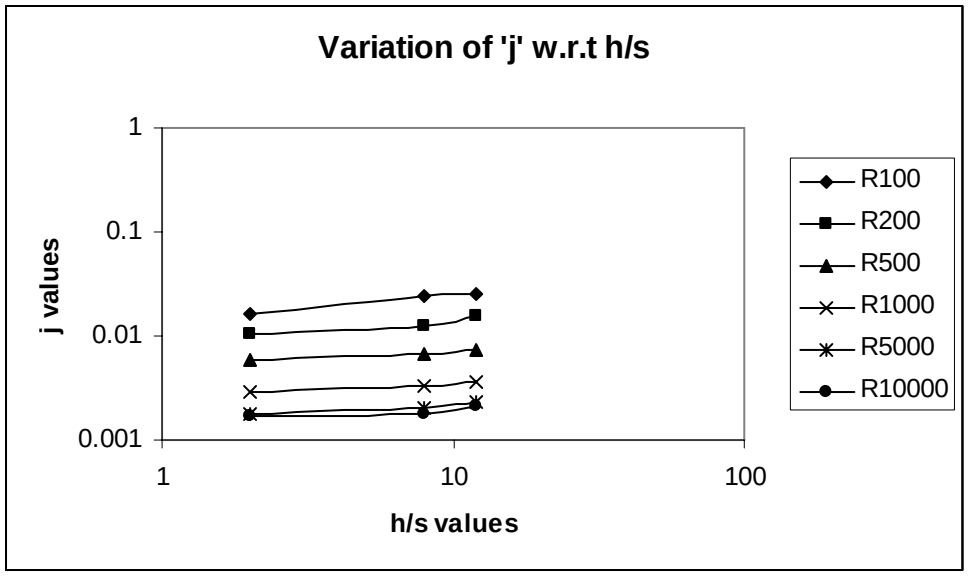

At a/s=.5 , l/s =16

In a manner, similar to that followed for plain and offset strip fins, it is intended to express these results in the form of simple correlations. It is proposed to seek the correlations in the form:

$$f \text{ or } j = C(\mathrm{Re})^{a0} \left(\frac{h}{s}\right)^{a1} \left(\frac{a}{s}\right)^{a2} \left(\frac{\Lambda}{a}\right)^{a3} \qquad (6.13)$$

Unlike the plain and offset strip fin geometries, it is seen that the **j** and **f** vs Re data for wavy fin surfaces show significant nonlinearity over the Reynolds number range 100<Re<10,000. Therefore, two separate equations have been proposed for the low and the high Re regimes. The following procedure has been employed to arrive at the correlations.

Determination of indices a1-a3 from numerical data

The j and **f** data given in Table 6.3 are analyzed in selected groups where all geometric parameters except one are kept constant at their average values. The results are plotted against the independent variable in log-log scale and the slopes determined. These slopes yield the values of a1 to a3 for each value of Re. The constants a1 – a3, thus computed are given in Table 6.4. It is observed that, unlike those for offset strip fin surfaces, the indices determined from single factor experiments with wavy fin geometry vary with Re by a significant extent.

The data have also been analyzed by multiple regressions to match eq (4.13), and the resulting coefficients presented in Table 6.5. The low values of the correlation coefficient R (0.95, 0.97) confirm the observations of the single factor experiments.

Table 4.1: Determination of indices a1 to a3 of eq (4.13) from single factor experiments.

Re	Friction factor f			Colburn factor j			
	a1	***a2***	***a3***	***Re***	***a1***	***a2***	***a3***
100	-.03299	-0.0275	-1.1599	100	0.2885	-0.4213	-2.2587
200	0.2388	-0.0729	-1.4119	200	0.1093	-0.2374	-1.7938
500	0.1066	-0.2294	-1.8127	500	0..0885	-0.1421	-1.5615
1000	0.064	-0.2502	-1.8833	1000	0.1097	-0.2933	-1.3896
5000	0.069	-0.4121	-2.5245	5000	0.0784	-0.3171	-0.7814
10000	0.0995	-0.4167	-2.1097	10000	0.0233	-0.3279	-0.5953

Chapter 5

CONCLUSION

- Contribution of this Thesis
- Possibilities of Future Work

5.1 Contribution of this Thesis

Plate Fin heat exchangers have already made a mark on the technology of the twentieth century. A variety of equipment – from automobiles to aircrafts, considers them essential, while others are adopting then for their superior performance. Still, the technology has remained largely proprietary. Driven by industrial needs and international sanctions, our country has initiated a multi–pronged research programme on this challenging subject. This thesis constitutes a small component of this effort.

. Issues related to materials, manufacturing techniques and design approaches remain crucial to widespread application of plate fin heat exchangers. Heat transfer and flow friction characteristics of plate fin surfaces , however, will play the most vital role in its success. There is a shortage of experimental data and all existing correlations essentially represent the same basic information.

The primary contribution of this thesis is twofold:

(a) It has introduced a new approach to developing heat transfer and flow friction correlations by combining computational and experimental data, and

(b) It has presented a new set of correlations for plain rectangular, offset strip and wavy fin surfaces - geometries that have found the maximum application.

Experiments on heat transfer over plate fin surfaces are expensive and difficultDirect numerical simulation (DNS) and comparable numerical techniques need computing resources beyond the affordability of most heat exchanger designers. Under these circumstances the approach taken in this thesis provides a workable solution. The general trends are computed by CFD, while a couple of constants are determined from experimental data.

Plain rectangular, offset strip and wavy fins are among the most commonly used fin types in cryogenic, aerospace and similar industries. This thesis provides heat transfer and flow friction correlations that should have wider applicability when compared with existing correlations

5.2 Possibilities of Future Work

With physical constraints on time and resources, we have not been able to address to some aspects of the problem which have a strong symbiotic relationship with the material covered in this thesis. Among the most obvious topics are:

1. Plain fins of non-rectangular geometry – triangular, trapezoidal and comparable shapes,
2. Offset strip fin in hard way configuration –
3. Herringbone fins
4. Other fin types such as perforated plain fins and louver fins. The louver fin, particularly, can offer substantial computational challenges.

Availability of better heat transfer and flow friction correlations and increased confidence in the results are expected to stimulate the application of these fin geometries .

Chapter 6

REFERENCES

1. **Maity, Dipak** Heat Transfer and Flow Friction Characteristics of Plate Fin Heat Exchanger Surfaces – A Numerical Study

2. **Kays, W. M. and London**, **A. L.** Compact Heat Exchangers, McGraw-Hill, New York (1984)

3. **Wieting**, **A. R.** Empirical Correlations for Heat Transfer and Flow Friction Characteristics of Rectangular Offset-Fin Plate-Fin Heat Exchangers *ASME J. Heat Transfer* **97** 488-490 (1975)

4. **Joshi, H. M. and Webb, R. L.** Heat Transfer and Friction of the Offset Strip-fin Heat Exchanger *Int. J. Heat Mass Transfer* **30(1)** 69-84 (1987)

5. **Manglik, R. M. and Bergles**, **A. E.** Heat Transfer and Pressure Drop Correlations for the Rectangular Offset Strip Fin Compact Heat Exchanger *Exp. Thermal Fluid Sc.* **10** 171-180 (1995)

6. **Muzychka, Y. S. and Yovanovich, M. M.** Modeling the **f** and **j C**haracteristics of the Offset Strip Fin Array *J. Enhanced Heat Transfer* **8** 243-259 (2001)

7. **London, A. L.** A Brief History of Compact Heat Exchanger Technology, in **R. K. Shah, C. F. McDonald and C. P. Howard (Eds),** *Compact Heat Exchanger – History, Technological Advancement and Mechanical Design Problems,* HTD, **10**, ASME, 1-4, (1980)

8. **Panitsidis, H., Gresham, R.D. and Westwater, J. W.** Boiling of Liquids in a Compact Plate-Fin Heat Exchanger, Int. J. Heat Mass Transfer, **18**, 37-42, (1975)

9. **Robertson, J.M.**, Boiling Heat Transfer with Liquid Nitrogen in Brazed – Aluminium Plate–fin Heat Exchangers, American Institute of Chemical Engineers Symposium Series, San Diego, **75**, 151-164 (1979)

10. **Lenfestey, A. G.** Low Temperature Heat Exchangers, in *Progress in* **K. Mendelsson (Ed)** *Cryogenics* **3,** 25-47, (1961)

11. **Shah, R. K. and Webb**, **R. L.** Compact and Enhanced Heat Exchangers, in **J. Taborek, G. F. Hewitt and N. Afgan (Eds),** *Heat Exchangers – Theory and Practice* McGraw Hill, New York, 425-468 (1983)

12. **London, A. L.** Compact Heat Exchangers – Design Methodology in **S. Kakac, R. K. Shah and A. E. Bergles (Eds),** *Low Reynolds Number Flow Heat Exchangers*, Hemisphere Publishing Corp. Washington DC, 21-27 (1983)

13. **Shah, R. K.** Compact Heat Exchanger Design Procedures, in **S. Kakac, A. E. Bergles and F. Mayinger (Eds),** *Heat Exchangers – Thermal-Hydraulic Fundamentals and Design,* Hemisphere Publishing Corp., Washington DC,495-536 (1981

14. **Shah, R. K.** Compact Heat Exchanger Surface Selection Methods in Heat Transfer1974, *Proceedings of the 5th International Heat Transfer Conference*, Hemisphere Publishing Co, New York, **4**, 193-199 (1978)

15. **Soland, J. G., Mack, W. N. and Rohsemnow**, **W. B.** Performance Ranking of Plate-fin Heat Exchanger Surface, ASME J. Heat Transfer (1978) **100**, 514-519